A COMPACT, RECONFIGURABLE UHF COMMUNICATION SYSTEM DESIGN FOR USE WITH POLYSAT'S EMBEDDED LINUX PLATFORM

A Thesis

presented to

the Faculty of California Polytechnic State University,

San Luis Obispo

In Partial Fulfillment

of the Requirements for the Degree

Master of Science in Electrical Engineering

by

Austin Williams

September 2013

COMMITTEE MEMBERSHIP

TITLE:	A Compact, Reconfigurable UHF Communication System Design for use with PolySat's Embedded Linux Platform
AUTHOR:	Austin Williams
DATE SUBMITTED:	September 2013
COMMITTEE CHAIR:	Dr. Dennis Derickson, PhD Department Chair of Electrical Engineering
COMMITTEE MEMBER:	Dr. Vladimir Prodanov Assistant Professor of Electrical Engineering
COMMITTEE MEMBER:	Dr. Jordi Puig-Suari Professor of Aerospace Engineering
COMMITTEE MEMBER:	Dr. John Bellardo Assistant Professor of Computer Science

ABSTRACT

A Compact, Reconfigurable UHF Communication System Design for use with PolySat's Embedded Linux Platform

Austin Williams

The beginning of this thesis provides an overview of the heritage UHF Communication System design flown on CP2, CP3, CP4, CP5, and CP6, summarizing previous analysis of its performance, and providing the justification for a complete system re-design. High level requirements for the new UHF System are defined, and a trade study is performed on state-of-the-art single chip transceivers, low noise amplifiers, and transmit power amplifiers. These components are then designed into a functional communication system, with key components analyzed for proper impedance matching and performance characterization compared to expected datasheet values. Next, the system as a whole is characterized for its receive sensitivity, and issues are documented that arose during this system testing. Performance of the new system demonstrate the dramatic improvement over the heritage design, but highlights the importance of a proper antenna design. Several charts produced from a simplified link budget using empirical data provide expected data rates given different orbital altitudes and transmit powers. Lastly, a brief discussion on future work for turning the system into a ground station, and the potential for dynamic on-orbit data rates to maximize the data down while minimize power requirements is discussed as future work.

ACKNOWLEDGMENTS

If I have seen further, it is by standing on the shoulders of giants. -Sir Isaac Newton

To the early CubeSat pioneers who knew they'd change the world, while the world thought their antics cute. To Dr. John Bellardo, for bringing this hardware to life. Sorry about those interrupts. To Dr. Jordi Puig-Suari, a true visionary and friend. Above all, to my parents Gregory and Linda, who shaped around me a world of opportunity.

TABLE OF CONTENTS

LIST OF TABLES

LIST OF FIGURES

1 Introduction

1.1 PolySat Background

Since the PolySat program began development of CP1 in 2000, the program has successfully integrated six spacecraft on four launch vehicles [1] [2]. Throughout the years, lessons learned from designing, building, testing, launching, and operating spacecraft has been passed on through the generations of students. The constant turnover of students presents an enormous challenge to custom spacecraft design. A large number of universities and organizations all over the world opt to buy off-the-shelf sub-system designs, rather than developing custom hardware. However, as an educational institution priding itself on a "Learn By Doing" philosophy, PolySat continues to develop all the satellite subsystems in-house.

Since the successful launch of CP6 in May of 2009 [2], senior members of the team turned our focus to a complete overhaul of the avionics system. The avionics system comprises everything but the experiment, or payload. Such an abrupt rework of an entire spacecraft is quite unusual in the aerospace industry since flight heritage of components and systems are so highly valued. However, the Electrical Power System [EPS] [5] and the Communications and Data Handling [C&DH] [3] were completed around the 2004 time frame, meaning the components are now 6 years old. One look at the rapid progression cell phone technology makes every 6 months makes 6 year old technology seem antiquated. If the smartphone boom is any indication, low power, mobile technology is in extreme demand. The intent of a full avionics overhaul is to reap the technological benefits of a thriving sector by repurposing it for an application it was, in fact, never designed for. The previous CP series of satellites and the CubeSat community as a whole have demonstrated that most of this technology works surprising well in a Low Earth Orbit [LEO].

While being a student run organization presents many challenges, it also has benefits. Aerospace companies and organizations are risk averse–hence the high value placed on flight heritage. The caution to take risks with component selection inevitably means satellite hardware will never keep up with the latest and greatest technology in consumer products. The CubeSat platform in the hands of fearless students offers a unique opportunity to change that paradigm–particularly when allowed to wipe the slate clean, and approach the system design from a fresh perspective. Board fabrication and assembly facilities are not prohibitively expensive for a sponsored project anymore.

Now, students can design in highly integrated chips with BGA and QFN interfaces, without worry of assembling them by hand. In fact, assembling a board only requires a good assembly drawing, and a bill of materials.

The new avionics system in development represents PolySat's second attempt to standardize the spacecraft electronics. The subsystem distribution is radically different than the previous generation in order provide flexibility for different mission requirements, improve noise isolation for RF Subsystems, and to maximize the payload space.

1.2 Scope of Thesis

While I lead the development of the entire Avionics package, this thesis will focus primarily on the UHF Communication System design and performance analysis in order to address known issues from the previous design. However, due to the highly integrated nature of this avionics package, some design choices were heavily influenced by the Embedded Linux Systemboard design, and vice-versa. Only high level design information about the Systemboard is discussed as it pertains to the UHF Communication System.

Section 2 provides a concise overview of the previous design. It starts by discussing the design requirements and constraints. It then discusses the overall communication system architecture.

Section 3 summarizes the known issues with the old design. An in depth study previously performed is also summarized with its conclusions drawn and recommendations for improvement. Additional comments are made about that studies results.

Section 4 discusses the new design requirements and constraints for the communication system under development.

Section 6 begins with a trade study on the key components. With the parts selected, an system overview is shown along with schematics with descriptions. The layout files are shown with an explanation of the board stack up design, and layout rules followed.

2 Summary of Heritage UHF Communication System

2.1 Design Requirements

The first fully custom PolySat avionics system has two basic, high level design requirements.

1. One-third of the Mass, Volume, and Power is reserved for the payload [3].
2. The system should be flexible enough to support various future payloads [3].

These straightforward requirements flow down to the subsystem design, imposing additional, more specific requirements given the constraints.

2.1.1 UHF Communication System Constraints

1. Limited communication window. A 650-700km altitude and a 98° inclination yields a worst case scenario of a single daily pass 5 minutes long [3][4].
2. Expected to operate over a temperature range from -30 to 70 degrees celsius [4].
3. Radiation from cosmic rays will interact with the electronics, and may cause Single Event Upsets (SEU) or Single Event Latch-ups (SEL) [4]. SEUs occur when an energetic particle from deep space passes through the semi-conductor constituting the component, ionizing the local area enough to logically flip a bit. The affect on the system largely depends on which bit is flipped. Re-writing the bit will clear the issue. SELs occur when a charged particle effectively creates a short circuit within the semi-conductor. These can only be cleared by temporarily removing power from the system. Failure to remove power could results in a complete hardware failure due to the short circuits.
4. The vacuum of space may affect the operation of our electronics [4].
5. Limited funds [4]. Financial assistance comes in various forms to the lab. However, fabricating and assembling boards is still a major cost of the program.
6. Limited power budget. CubeSats are inherently surface area limited, which restricts the number of solar cells assembled on each side panel. Additional surface area could be provided using deployable panels, but this greatly increases the complexity of the design. The CP2 Electrical Power System design [5] provides 8.8 W*hrs of battery capacity, and a calculated available orbit average power of 1.1W. This power is shared amongst all the subsystems, with

the communication system requiring the most power due to the RF amplifier, and reasonably high duty cycle from the periodically transmitted beacon.

2.1.2 UHF Communication System Derived Requirements

1. Implement a simple beacon. After ejection from the Poly Pico-Satellite Orbital Deployer (PPOD), students must somehow track the satellite. Based on experiences from the japanese CUTE-1 satellite [11], an audible morse code beacon, followed by an AX.25 packet containing basic satellite health telemetry is invaluable as quick acquisition of the satellite overhead makes better use of the limited communication window. [4].

2. A 1200baud data rate requirement was derived based on the CP2 mission requirements. It was estimated that 40kB of total data is required for the mission. Given worst case conditions of a single 5 minute pass per day, a data rate of just over 1kbps is required. Since standard data rates are based off multiples of 300bps, a 1200baud data rate was selected [4].

3. Maximize reliability. It was decided to design a fully redundant UHF System to avoid single points of failure [4] [3].

4. Minimize hardware cost. Avoiding space rated components dramatically reduces the cost of hardware. Additionally, Commercial Off the Shelf (COTS) parts are more readily available with great support [4] [3].

5. Minimize power consumption. Care in component selection can greatly reduce the communication subsystems power requirements. The peak power consumption is not to exceed 3.5W [4] [3].

6. The satellite must comply with FCC regulations and capable of operation with a modestly priced ground station. [4] [3].

7. To help meet the volume requirement, hardware should be replaced with software where possible. Off the shelf systems should be avoided as they contain a lot of peripherals and functionality that are not necessary. Designing the system at the IC level and combining subsystems onto single boards optimizes volume [3].

2.2 Hardware Overview

The PolySat team at the time decided on a two board stack design. The Power Board provides the the Electrical Power System (EPS), which contains the power regulators, batteries, and interfaces to the side panels with solar cells. The Communication & Data Handling (C&DH) board provides the redundant communication subsystems along with the Telemetry, Telecommand & Control System (TT&C). The TT&C processes commands received from the communication subsystem, controls data flow, and collects health telemetry from the spacecraft.

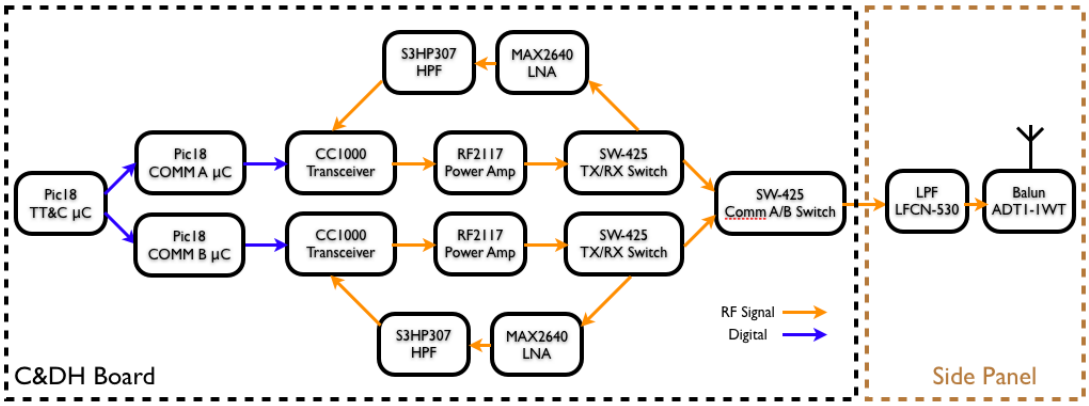

Figure 1: Overview diagram of heritage communication system flown on CP6.

A simplified overview of the C&DH board is shown in Figure 1. The TT&C is implemented within a very low power Pic18 Microcontroller, and uses an I^2C data interface to two addition, redundant Pic18 microcontrollers running identical firmware. These redundant Pic18's, called the COMM Pics, provide the Terminal Node Controller functionality, which is responsible for building the AX.25 packets, and sending them to the transceiver for transmission at the proper data rate over a single data line interface to the CC1000 while clocked to a 1200 baud signal generated by the CC1000. This is sometimes called a wire mode interface, where all digital data sent to the CC1000 is transmitted over the air. At each bit-time clock edge, an interrupt triggers the software TNC within the COMM Pic to process the bit. Registers in the CC1000 control the frequency, modulation scheme, data rate, transmit power, encoding type, and various other parameters. The CC1000 is setup to use Frequency Shift Keying (FSK). These registers are programmed by the COMM Pics over a 3 wire data interface shown in Figure 2. The CC1000 has a built in TX/RX switch, so there are dedicated pins for transmit and receive. The RF2117 is a power amplifier, providing around 1W of RF power out. An antenna is switched between the two transmit paths, and two receive paths by using three SW-425 RF Switches. The antenna and matching circuitry are on a separate board. The C&DH

board provides a 50Ω U.FL coax connection that is run to the side panel that the dipole antenna is mounted to. Along with the antenna, the side panel provides a Balun to eliminate commode mode currents on the coax shield, and a Low Pass Filter to limit spurious signals from the power amplifier. The receive path has a MAX2640 Low Noise Amplifier and a S3HP307 High Pass Filter. These parts were added to the receive line in an attempt to fix the uplink issues experienced with CP3 and CP4 [1].

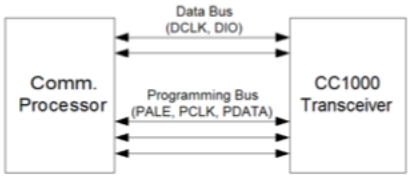

Figure 2: CC1000 digital interfaces to the Pic18 Microcontroller running the software TNC. When transmitting, all bits on Data Bus get transmitted over the air. The Programming Bus controls internal registers.

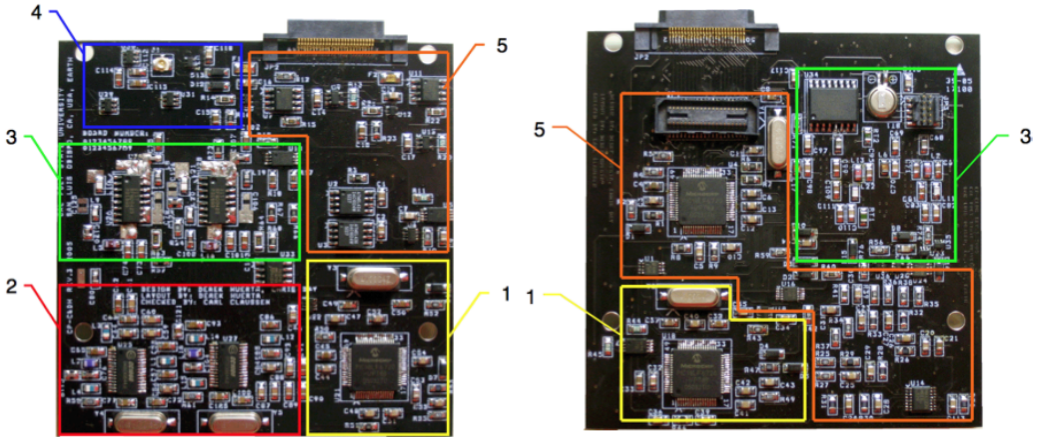

(a) Top of C&DH Board **(b)** Bottom of C&DH Board

Figure 3: Images of C&DH boards flown on CP3 and CP4

1	Pic 18 COMM Microcontrollers
2	CC1000 Transceivers
3	RF2117 Amplifiers
4	RF Front End
5	TT&C Subsystem

Table 1: Legend for Figure 3a and 3b

3 Motivation for UHF Communication System Redesign

3.1 Heritage UHF Communication System Known Issues

Soon after first contact with CP3 and CP4, it became apparent that the receivers on both systems were not reliably hearing commands sent from the ground. The PolySat team has since been working to resolve the issues seen on orbit. Essentially, the transmit path for the UHF System works very well, but the ability to receive is unreliable. Commands occasionally do get through, but not with any regularity. On occasion, 3 or 4 commands in a row could get uplinked, and at other times, two weeks can pass without contact. The difficulties experienced in operating a satellite with poor uplink make the Dnepr 1 crash in 2006 that much more frustrating. CP1 and CP2 were both lost in that wreck. While CP1 flew hacked apart Alinco DJ-C4 transceivers, CP2 flew the UHF System in question. Had CP2 made it to orbit, recognition of these uplink issues could have lead to changes in the CP3 and CP4 UHF Systems that may have increased the mission data throughput.

3.1.1 CP3 and CP4 Performance

The UHF System flown on these satellites is similar to the diagram shown in Figure 1, except the LNA and the HPF on the receive lines were not yet designed in. A number of theories were thrown around, but it's ultimately agreed that the receive sensitivity of both spacecraft is quite poor. Several students, with the help of an alumni, were able to travel with ground station equipment up to SRI in Palo Alto, CA, to use their 60 foot dish. At 430Mhz, this dish provides 35dB of gain with a 3° beamwidth. It can track the azimuth at 5°/sec and elevation at 2°/sec, allowing us to track a spacecraft in LEO. The ground station in our lab uses dual phased yagi antenna's, providing around 18.95dBi of gain [2]. With all other ground station equipment being equal, this test effectively added 17dB of gain to our uplink budget. Even so, improvement was surprisingly marginal.

3.1.2 CP6 Performance

During the development of CP6, the team agreed to add a High Pass Filter and a Low Noise Amplifier to the receive line. The HPF completed an effective Band Pass Filter when put in series with the LPF at the antenna to help prevent receiver saturation, which could result in harmonic generation, and potential jamming.

While on orbit, CP6 did show an improvement in uplink reliability, but it clearly did not solve the issue. This prompted Ivan Bland, an Electrical Engineering graduate student, to write a thesis

studying the problem [2]. It was clear the PolySat lab did not have a means of accurately measuring the receive sensitivity of the satellite. While long range testing was done on Bishops Peak to simulate the path loss, no actual measurements of the power reaching the LNA front end are made. When long range testing is done on two different revisions of the UHF System, something can be said about the relative performance of the two systems with a rather large margin of error, but the absolute sensitivity cannot be measured without sampling the received signal.

3.2 Summary of Previous Analysis Performed

The contents of this section summarize the results from Ivan Bland's thesis [2]. More information on data points and observations contained in this section can be found in Ivan's analysis.

3.2.1 Method of Receive Sensitivity Measurement

The heart of the analysis requires an accurate, repeatable method of measuring the receive sensitivity. Figure 4 shows the test setup that Ivan developed.

A The Yaesu FT-847 is an amateur radio transceiver. The Rigblaster interfaces the audio from the Computer to the radio by controlling the Push To Talk (PTT) line when transmitting. MixW is a software TNC that encodes and decodes AX.25 packets. When transmitting, serial data within the computer is run through MixW, which builds the TNC packet, and generates the Audio Frequency Shift Keyed (AFSK) signal. The AFSK signal is sent out of the sound card through the Rigblaster, into the Yaesu radio Mic port. The Rigblaster triggers the PTT line, resulting in the Yaesu radio up-mixing the audio to the carrier frequency for transmission. Receiving a signal works essentially in the opposite, where the Yaesu down-converts to audio, which is ultimately fed to the MixW for decoding as AFSK.

B A 30dB Attenuator, and a Variable Attenuator in series, The Variable Attenuator is ultimately used to control the signal power into the Device Under Test (DUT).

C 3dB splitter sends equal power signals to the Spectrum Analyzer and DUT. The signal strength read off the Spectrum Analyzer is the same signal strength seen by the DUT, allowing absolute measurements of the receive sensitivity.

D HP 8566B Spectrum Analyzer with a 43.2dB LNA on the front end. Similar to the addition of the LNA onto the front end of CP6, this greatly lowers the noise floor of the spectrum analyzer by reducing the Noise Figure of the input. The default configuration for the Spectrum Analyzer

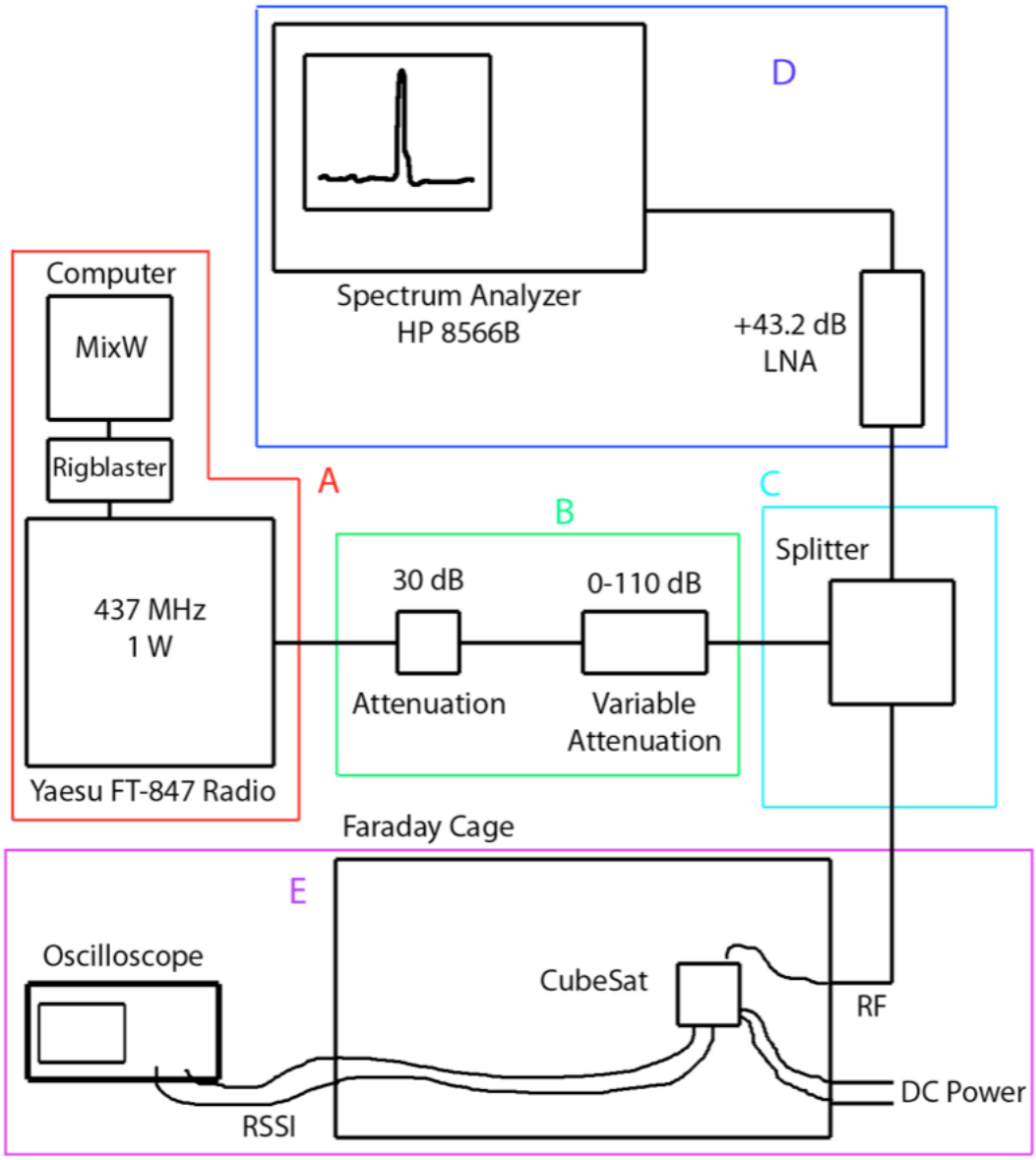

Figure 4: Overview diagram of test setup to measure the receive sensitivity of a communication system [2].

results in a Noise Figure of 43.23dB. By adding the LNA on the front end with a measured noise figure of 3.127dB, the cascaded Noise Figure is reduced to 5.58dB. In this configuration, it was found capable of measuring signals down to -120dBm.

E Oscilloscope to measure the Receive Signal Strength Indicator (RSSI) pin on the CC1000. This outputs an analog voltage inversely proportional to the signal strength at the Intermediate Frequency (IF) of 150kHz with $\pm$ 6 dB accuracy. The Faraday Cage is a custom built box designed to fit a 3U cubesat. It's constructed with cheap copper clad PCB's and provides 70dB

of attenuation. The cage must sufficiently attenuate the stray RF emanating from the Yaesu radio as to not wirelessly communicate with the DUT within the faraday cage. 70dB proved sufficient. Additionally, various RF and DC feed throughs allow power to the DUT, and a carefully controlled RF input.

3.2.2 Simplified Link Budget Calculations

A worst case link budget was performed for both the uplink and downlink for a 700km orbit with a 98° inclination. The table from Ivan's thesis is reproduced below:

Parameter	**Magnitude**	**Comments**
P_{TX} (Amplifier Output)	30dBm	RF amp produces 1W
G_{TX} (Isotropic Antenna Gain)	+2 to -10dBi	Depends on orientation
L_{FS} (Free space path loss)	-142.2 to -153.4dB	700km to 2500km slant range at 5° elevation
L_M (Miscellaneous loss)	-1dB	Estimated additional loss (Connectors, radio, etc.)
L_{RX} (5/8" hardline loss)	+18.95dBi	Antenna Gain
Total	$\mathbf{-90 to -113 dBm}$	Approximate strength after antenna (rounded)

Table 2: Simplified downlink budget for 700km orbit at 98° inclination.

Parameter	**Magnitude**	**Comments**
P_{TX} (Amplifier Output)	+50dBm	100W to the Ground Station Antennas
G_{ANT_TX} (Isotropic Antenna Gain)	+18.95dBi	16.8dBd + 2.15dB = 18.95dBi
G_{PHS_TX} (Gain from dual phasing)	+3dB	Dual phased antennas provide additional gain
L_{TX} (5/8" hardline loss)	-0.22dB	50 ft length
L_M (Miscellaneous loss)	-1dB	Estimated additional loss (Connectors, radio, etc.)
L_{FS} (Free space path loss)	-142.2 to -153.4dB	700km to 2500km slant range at 5° elevation
G_{RX} (Antenna gain of satellite)	+2 to -10dBi	Approximate strength of antenna (rounded)
Total	$\mathbf{-70 to -93 dBm}$	Approximate strength after antenna (rounded)

Table 3: Simplified uplink budget for 700km orbit at 98° inclination.

3.2.3 Summary of Measured Results and Conclusions

Board	Sensitivity		Comments
	CommA	CommB	
CP3 and CP4 Revision	-89dBm	-92dBm	No LNA or HPF on the front end
CP6 Revision Board 1	-94dBm	-101dBm	Added LNA and HPF
CP6 Revision Board 2	-96dBm	-100dBm	Added LNA and HPF
Yaesu FT-847	-115dBm		Ground Station Transceiver

Table 4: Result of measurements taken on two revisions of C&DH board. The improved receive sensitivity as a result of the LNA shows a 5 to 9dB improvement from the CP3 and CP4 version, to the CP6 version.

Noise Floor of Receive Line: Table 5 below shows the measured values of the noise floor on several different boards using the CC1000. A slightly higher noise floor is seen on the CP3 and CP4 revisions. Stronger crystal harmonics were noticed. Broadband noise is generally attributed to a non-ideal layout.

CommSystem	NoiseFloor	Comments
CP3 and CP4 Revision CommA	-107.3dBm	Measured Sensitivity: -88.5dBm
CP3 and CP4 Revision CommB	-112.3 dBm	Measured Sensitivity: -92.4dBm
CC1000 Development Board	-117.3 dBm	Provides proper layout comparison
System Noise Floor	-127.3dBm	Noise Floor of spectrum analyzer with LNA

Table 5: Noise Floor values at the receive frequency with Spectrum Analyzer set to 1Mhz span and 10kHz Resolution Bandwidth.

CommSystem	NoiseFloor	Comments
CP3 and CP4 Revision CommA	-92.3dBm	Measured Sensitivity: -88.5dBm
CP3 and CP4 Revision CommB	-102.3dBm	Measured Sensitivity: -92.4dBm
CC1000 Development Board	-102.3dBm	Provides proper layout comparison
System Noise Floor	-112.3dBm	Noise Floor of spectrum analyzer with LNA

Table 6: Broadband Noise Floor values with Spectrum Analyzer set from 100 - 500Mhz with a 1Mhz Resolution Bandwidth.

Switching Noise form DC/DC converters: One theory said the switching noise of the regulators feeding the CC1000 may attribute to reduced sensitivity. However, powering the CC1000 directly from a low noise linear power supply showed no improvement in sensitivity.

Switching Noise from I^2C Bus: The avionics package uses I^2C operating at 100kHz extensively through the system. Since the CC1000 operates as a typical Heterydyning transceiver with an I_f at 150kHz and a passband of 175kHz, I^2C noise could interfere with the CC1000. However, sensitivity measurements with the I^2C bus inactive shows no improvement.

Long Duration Testing: The Comm boards occasionally don't respond to commands even with adequate signal strength. This occurs randomly, and is thus difficult to study. However, a long duration test can help characterize this. The satellite was setup connected to the ground station, and fed a -50dBm signal. Flight Code was used on the unit, and the computer sent a command asking the satellite to "Beacon" with a response. Over three days, the results are tabulated in bins, showing the time between beacon's, allowing us to determine how many commands were sent between responses. The first bin of 90 seconds represents commands correctly decoded on the first attempt. The second bin means two commands were sent, third bin means three commands, etc. Figure 5 shows that even under ideal conditions (no temperature swings or doppler shift, strong signal to noise ratio) the spacecraft occasionally won't decode properly. This likely is a software issue.

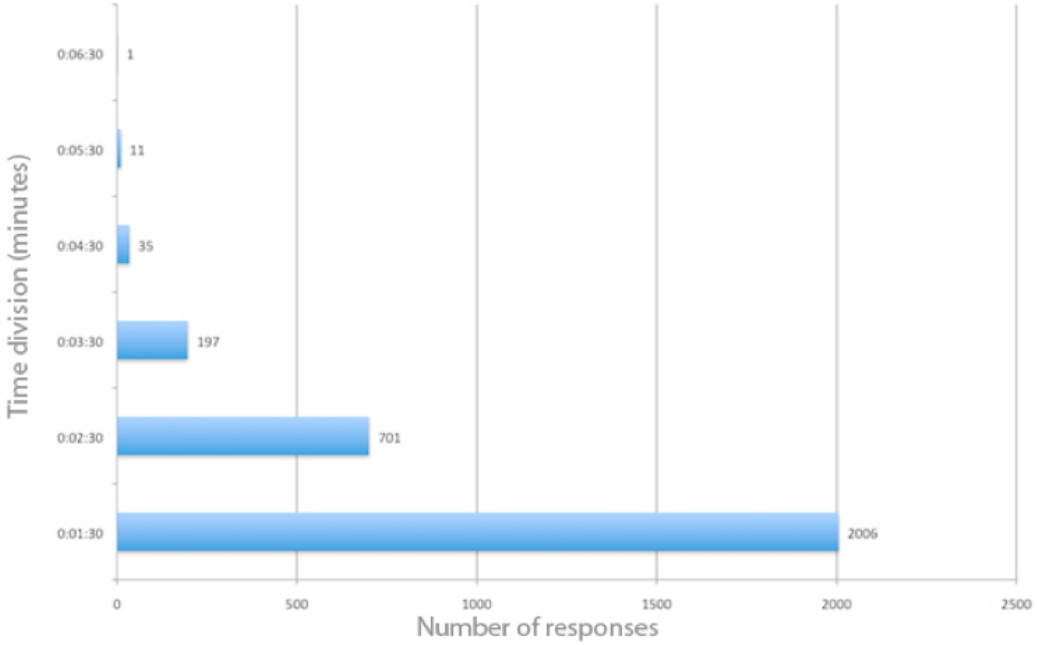

(a) Histogram of 3 day Long Duration Test

Test Duration	70 Hours
Commands Sent	4199
Acknowledgments	2952
Successful Uplink	70.3%

(b) Long Duration Results

Figure 5: Histogram of 3 day Long Duration Test. Different bins indicate how much time passed between acknowledgments of commands sent every 60 seconds. This test shows, under ideal conditions, the satellite still misses commands almost 30% of the time.

Crystal Oscillator Temperature Dependence: Cheap crystals were used in the original design with tolerances on the order of 30ppm. Calculations performed based on application note AN019 from Ti are reproduced in Figure 7 below. The IF is centered at 100kHz, with a 175kHz passband. As the IF frequency is shifted near the edges of the passband, signal distortion and reduced sensitivity may result.

Item	Value	Units
Initial Tolerance ±	30	ppm
Temperature Drift ±	50	ppm
Aging ±	5	ppm
Load Error	2	ppm
Total	*87*	ppm
Worst Case Frequency Error TX ±	35.2	kHz
Worst Case Frequency Error RX ±	35.2	kHz
Worst Case IF Error ±	70.3	kHz

Table 7: Calculation of worst case crystal frequency errors.

3.2.4 Recommendations for Improvement

1. Select a transceiver with a better receive sensitivity and more robust RF synthesizer.
2. Improve the layout to reduce broadband noise and crystal harmonics. Follow manufacture suggested part placement and layout where possible.
3. Long duration testing should play a major part in the software development.
4. Use a temperature controlled crystal oscillator for the RF synthesizer within the chosen transceiver chip to reduce frequency offset errors.
5. Proper testing procedures for RF chain on assembled boards.
6. Careful use of U.FL connector. These tiny 50Ω RF cables get easily damaged.
7. Contract for professional board assembly to eliminate solder workmanship issues.
8. Ground Station upgrades. Higher power amplifiers are available (1000W), but expensive and should not be necessary. They are available is a contingency.

3.3 Additional Comments on Analysis and Measurements Previously Performed

3.3.1 Front End Filtering

In hindsight, the front end bandpass filter is ineffective for blocking spurious signals on the receive line. The S3HP307 HPF has a -3dB cutoff at 300Mhz. The LFCN–530 LPF has a -3dB cutoff at 530Mhz. This gives a passband of 230Mhz. At the time, this was tightest filtering that could be done given the schedule, and experience of the students working on the problem. Since LNA's are fairly broadband even when matched to a particular frequency, it still stands susceptible to some level of saturation from spurious signals around 400MHz.

3.3.2 Front End Noise Figure

The noise figure at the front end of a RF chain sets the system noise figure. With the CP3 and CP4 design, the CC1000 sets the noise figure since only the internal LNA is used. At 433MHz, the CC1000 has a cascaded noise figure of 12dB [9]. In order to estimate the cascaded noise figure with the LNA added, equation 1 is used.

$$F_{cascade} = F_1 + \frac{F_2 - 1}{G_1} \tag{1}$$

The measured noise figure and gain of the MAX2640 is 2.3dB and 14.8dB respectively [1]. To use Equation 1 above, we must convert the numbers from dB, to a linear multiplier, and plug in:

$$\begin{aligned} F_1 &= 2.3dB = 10^{\frac{2.3}{10}} = 1.698 \\ F_2 &= 12dB = 10^{\frac{12}{10}} = 15.850 \\ G_1 &= 14.8dB = 10^{\frac{14.8}{10}} = 30.200 \\ F_{cascade} &= 1.698 + \tfrac{15.850-1}{30.2} = 2.190 \\ \mathbf{F_{cascade}} &= \mathbf{10log_{10}(2.190) = 3.4dB} \end{aligned} \tag{2}$$

For a system requiring the reception of faint signals pushing the limits of the receiving capability of the chip, a 3.4dB cascaded noise figure on CP6 could be better, but it's a nice improvement over the 12dB noise figure on CP3 and CP4.

3.3.3 Test Bed Conditions vs On Orbit Environment

The downlink of our satellite has proven reliable. The downlink budget shown in Table 2 gives a worst case received signal of -113dBm, which gives a link margin of only 2dB. On orbit, we notice the link approaching, and likely passing this worst case scenario when in the middle of a data dump, the spacecraft rotates so the null of the dipole points to the ground station, and packets are lost. After a brief time, the signal strength returns, and packets reception resumes. The uplink appears to show decent margin under the worst case scenario defined in Ivan's thesis. With a receive sensitivity of -100dBm, and a worst case signal strength of -93dBm after the antenna, that gives 7dB of margin. However, a few factors could make these receive sensitivity values optimistic for real world operation.

1. The receive sensitivity measurements are performed in an ideal environment, where the noise subjected to the DUT is purely conductive. In reality, while orbiting in LEO, the spacecraft is subjected to radiated RF from a multitude of man made objects, as well as cosmic background radiation. Additionally, a system with a flight antenna may be affected by internal electrical EMI issues through capacitive and/or inductive coupling in the near field of the antenna.

2. Frequency offset from the carrier as a result of inaccurate doppler shift compensation, and thermal cycling of the crystal.

3.3.4 Frequency Offset Calculation

The calculation for frequency offset due to crystal error in Section 3.2.3 does not take into account error in doppler correction. The ground station compensates for the doppler shift. However, inaccuracies in the orbital knowledge of the spacecraft will cause errors in doppler shift on the order of a few kHz at most. Additionally, the calculation assumes both the transmitter and receiver use the same crystal, which is not true. The Yaesu FT-847 radio provides a frequency stability better than ± 2 ppm [10] with very little temperature drift. Overall, the actual frequency offset should be better than what's calculated in Section 3.2.3.

3.3.5 Power Amplifier Availability

The RF2117 originally designed into the communication system is no longer in production. Sources for this component are scarce, and expensive. While technical reasons call for a new Transceiver, logistical reasons call for a new RF Amplifier.

4 New UHF Communication System Design Requirements

4.1 New High Level Avionics Design Requirements

As is natural, CubeSat missions continue to grow in ambition. The new avionics package development took the following high level design requirements:

1. Maximize the volume available to the payload.
2. Take advantage of the latest in microelectronics.
3. Flexibility for future payloads.

4.1.1 New UHF Communication System Constraints

The constraints for this design are essentially the same as in Section 2.1.1 for 1-5. The primary difference comes with line item 6, the limited power budget. The calculated orbit average power generation is closer to 1.6W in reality. This stems from the increased solar cell efficiency when coming out of eclipse as the solar cell temperature has dropped substantially. CP3, CP4, and CP6 have shown to be extremely power positive, and the battery voltages rarely dropped below 3.9V, indicating a state of charge around 90%.

4.1.2 Systemboard Requirements (as pertaining to UHF System)

1. A single board (called the Systemboard) will run Embedded Linux.
2. The AX.25 encoding takes place within the Linux environment.
3. Two generic daughterboard slots for communication systems, or payload electronics are available
4. Dedicated power regulators to each daughterboard slot with adjustable output voltages from 1.8V to 5.0V with a minimum output power of 5W.
5. Unregulated battery power to the daughterboards.
6. Low power, 3V3 power rail available to the daughterboards for sensors and logic.
7. SPI, I2C, UART, Hardware Interrupts, and several GPIO's should also be available.
8. Allow for power negative mission designs with large battery capacity, where several orbits for recharging batteries would get built into the mission operation plan.

4.1.3 New UHF Communication System Requirements

1. The RF Subsystem is designed onto a 83mm x 36mm daughterboard, allowing easy noise isolation, and filtering of all signals to minimize spurs, and lower the noise floor as much as possible.
2. The Daughterboard should allow for an RF cage to be soldered on.
3. Adjustable transmit power up to 2W.
4. Transceiver with flexible modulation scheme, data rates, filtering, operating frequency, and receive sensitivity superior to the CC1000.
5. Transceiver data rate of 9600 baud on the 70cm band (437Mhz), compatible with the current ground station at a minimum.
6. System Noise Figure better than 3.4dB (from Equation 2).
7. Improved front end filtering.
8. Reliable Receive Sensitivity better than -115dBm to match current ground station transceiver shown in Table 4.
9. UHF System redundancy is not forced. The 2nd daughterboard slot, if used, would operate on a different band.
10. The UHF System, with a possible minor board revision and tuning, could operate on the 915Mhz ISM band.
11. The design will take all recommendations from Section 3.2.4 into consideration.
12. Minimize power where possible.

5 Design Methodology and Trade Study

The budget allocates a maximum of three revisions for this design. Extensive analysis and simulation is not performed on the UHF System design. Instead, with the requirements in hand, a part trade study is performed, and components are selected that meet or exceed all requirements. These components are designed into a board with the final form factor and proper interfaces with the Systemboard using the reference designs typically included with the datasheet. After the boards have been fabricated and assembled, careful tuning of the matching networks will take place. A high priority is placed on providing functional hardware so software development can proceed in parallel with board tuning. While Figure 1 provides an overall system model, the details of the design are left till after the trade study is performed. Given the highly integrated nature of many of these devices, a particular component could have a major impact on the system design.

5.1 Trade Studies

The follow section provides comparisons of key features for various components, and explanations of why particular components are selected over others.

5.1.1 Transceivers

The transceiver will play the biggest role in determining the system design as it defines the data interfaces with the primary computer, the RF interface to the Receive and Transmit front ends, the capable operating frequencies for future board tuning, and packet formation.

Features	SI4431	CC110FX	ADF7021	*AX5042*	CC1000
Temperature Range (C)	-40 to +85	-40 to +85	-40 to +85	-40 to +85	-40 to +85
Frequencies (MHz)	240 to 930	315 to 915	80 to 650, 862-950	400 to 470, 800 to 940	300-1000
Modulation	FSK, OOK	FSK, MSK, OOK	FSK, 3FSK (Vertibi), 4FSK, MSK	FSK, MSK, PSK, OQPSK	FSK, OOK
Spectral Shaping	Gaussian	Gaussian	Gaussian and Raised Cosine	Gaussian	–
Data Rates (kbps)	1 to 128	1.2 to 500	0.01 to 32.8	1.2 to 600	0.6 to 76.8
Receive Sensitivity (dBm)	-118 [1]	-110 [6]	-121 [10], -129 [11]	-123 [14]	-110 [18]
Phase Noise (dBc/Hz)	-80 [2]	-92 [7]	-103 [12]	-85 [15]	–
	-90 [3]	-93 [8]	–	-80 [16]	-85 [19]
	-115 [4]	-107 [9]	-124 [13]	-105 [17]	–
Frequency Resolution (Hz)	156.25, 312.5 [5]	396.7	<433	1	250
RX Bandwidth (kHz)	2.6 to 620	54 to 750 (16 steps)	12.5 to 25	4.8 to 600	175
RSSI Resolution (dB)	±0.5	±0.5	±3	0.625, 0.1	±6
Receive Mode Power (mW)	55.5	59.4	79.2	52.5	28.8

Table 8: Trade Study for Transceivers showing key Features

SI4431: This transceiver from Silicon Labs has an impressive set of features. Antenna Diversity is supported within the chip, providing RF interfaces for each antenna. During the Pre-amble, the transceiver switches between the two antennas to determine which signal is more likely to decode properly. Since it has dedicated TX and RX pins, an external switch is not necessary to interface with the RF front ends. The RX bandwidth is very flexible, with data rates up to 128kbps. A major draw back are limited modulation schemes as it only supports FSK and OOK.

CC1000FX: A very interesting option as it is actually a System-on-Chip with a low power 8051 microcontroller at its core. This allows for a lot of interesting capabilities like automatic forward error correct (FEC) and 128-bit AES data encryption. Data rates up to 500kbps is very impressive, and support for MSK is nice as it's used often in the amateur radio world. The major

[1] BER $<$ 0.1% 2kbps GFSK with BT=0.5 and frequency deviation of 5kHz
[2] Δf=10kHz over the carrier frequency range (Datasheet isn't clear)
[3] Δf=100kHz over the carrier frequency range
[4] Δf=1MHz over the carrier frequency range
[5] 156.25Hz/step for 240-480Mhz, 312.5Hz/step for 480-930Mhz
[6] BER $<$1% at 1.2kbps GFSK with frequency deviation of 5.2kHz and 58kHz RX Bandwidth
[7] Δf=50kHz with f_c=400Mhz
[8] Δf=100kHz with f_c=400Mhz
[9] Δf=1MHz with f_c=400Mhz
[10] BER=10^-3 at 1kbps GFSK with frequency deviation of 1kHz and a 12.5kHz RX Bandwidth
[11] BER=10^-3 at 0.1kbps GFSK with frequency deviation of 1kHz and a 12.5kHz RX Bandwidth
[12] Δf=10kHz with f_c=433Mhz
[13] Δf=1MHz with f_c=433Mhz
[14] BER=10^-3 at 1.2kbps FSK
[15] Δf=50kHz with f_c=433Mhz
[16] Δf=100kHz with f_c=433Mhz
[17] Δf=2MHz with f_c=433Mhz
[18] BER=10^-3 at 2kbps FSK with frequency deviation of 32kHz
[19] Δf=100kHz over the carrier frequency range (Datasheet isn't clear)

drawback, and the deciding factor to not use it, is the receive sensitivity is significantly worse than the other options, and on par with the CC1000 at -110dBm. The performance is likely limited due to the integration of the 8051 microcontroller, and the associated noise.

ADF7021: Supports the best receive sensitivity, likely a results of its superior phase noise at the output of the frequency synthesizer. If the data rate is lowered to 100bps, the datasheet claims it can do -129dBm. Also some good options for modulation schemes including MSK, and the addition of Raised Cosine filtering of the baseband signal, although Gaussian filtering is sufficient. It requires the most power of all the transceivers at 79.2mW, with the worst RSSI resolution of ± 3 dB, though still better than the CC1000. The major drawback is the peak data rate of only 32.8kbps.

AX5042 : This chip is made by Axsem, a relatively new European company. Aside from the CC1000, it provides the lowest operating power in receive mode. Although the CC1000 uses only 28.8mW, the old design utilized two of them, requiring slightly more power than a single AX5042 chip. Additionally, it provides by far the best modulation options. This is the only chip I came across operating with these bands that can use PSK and OQPSK, in addition to MSK and the common FSK. It's capable of higher data rates than any of the other chips with extremely flexible filtering, and frequency programming in 1Hz steps. The frequency sensitivity for 1.2kbps is about the same as the ADF7021, however, the sensitivity does not increase below 1.2kbps. Overall, the AX5042 was selected as the transceiver since it provides a significant upgrade to the CC1000 using typical amateur radio data rates of 1.2kbps and 9.6kbps, with considerable flexibility for future UHF System requirements..

5.1.2 RF Amplifiers

The requirements for having an adjustable transmit power up to 2W while operating on both the 437Mhz amateur radio band and the 915Mhz ISM band turned out to be extremely restricting. The only readily available component that fit the bill is the RF5110G from RFMD, the same manufacture that made the obsolete RF2117 in the prior design.

From Table 9, we see that the RF5110G performs about the same as the RF2117, except for the higher transmit power, and the broad frequency range. With a chip rated to 4W, with proper thermal considerations, a 2W transmit seems reasonable.

Features	**∗RF5110G∗**	**RF2117**
Temperature Range (C)	-40 to +85	-40 to +85
Operating Frequency (MHz)	150 to 915Mhz	400 to 500
Efficiency	50 to 57%	>50
Gain	32dB of Gain with Analog Gain Control	33dB Small Signal Gain
Peak Transmit Power	+36dBm (4W)	33dBm (2W)
Supply Voltage	2.7 to 4.8V	3 to 5.5V

Table 9: Trade Study for RF Amplifiers showing key features

5.1.3 Low Noise Amplifiers

The low noise amplifier plays an important roll in conditioning the received signal by amplifying it, while adding the least amount of noise possible.

Features	**∗RF2373∗**	**ADL5521**	**MGA − 68563**	**MGA − 62563**	**MAX2640**
Temperature Range (C)	-40 to +85	-40 to +85	-40 to +85	-40 to +85	-40 to +85
Frequencies (GHz)	0.4 to 4	0.4 to 4	0.1 to 1.5	0.1 to 3	0.3 to 1.5
Gain (dB)	21.5	20.3	16.6	22	15.1
Max Input RF (dBm)	+15	+20	+21	+21	+5
Isolation (dB)	23	23.8	21.9	27.5	40
Noise Figure	1.1	0.8	1	1.25	0.9
Power (mW)	15	81	15	180	10.5

Table 10: Trade Study for LNAs showing key Features

A quality low noise amplifier can go a long way to improve the receive sensitivity of the system. From Table 10 above, we see that many options exist that are superior to the MAX2640 used in the previous design. The best options also require a significant amount of power. The ADL5521 provides a fantastic noise figure of 0.8dB with a gain of 20.3dB. However, at 81mW, this is a significant amount of power given the very high duty cycle it's expected to operate at. The MGA-62563 is slightly more gain at 22dB with a slightly high noise figure at 1.25, but even higher power requirements at 180mW. The MGA-68563 is comparable to the previously used MAX2640. The RF2373, compared to the ADL5521, provides more gain with 21.5dB, a slightly worse, but still respective noise figure of 1.1dB, but a significantly lower power requirements of only 15mW. For these reasons, the RF2373 is chosen.

5.1.4 RF Filters

Front end filtering at the RF frequency primarily prevent spurious signals from saturating the LNA and producing additional harmonic spurs. To accomplish this, a narrow filter around the carrier frequency is desired. As discussed in Section 3.3.1, the current filter scheme is ineffective with a passband of 230MHz. On the new design, a much tighter filter is researched. SAW filters provide

excellent narrowband filtering with a small form factor, and a reasonable insertion loss. Table 11 below summarizes the available SAW filter options.

Features	∗**MA09629**∗	**MA09155**	**SF0433020**	**LFCN530** and **S3HP307L**
Temperature Range (C)	-40 to +85	-30 to +72	-30 to +72	-40 to +85
Center Frequency (MHz)	435Mhz	433	433	415
Pass Band (MHz)	18	22.9	22.9	230
Max Input RF (dBm)	+10	+10	+10	+21
Insertion Loss (dB)	2.3	1.4	1.4	0.81 + 0.3
Max Input Power (dBm)	+10	+10	+10	–

Table 11: Trade Study for SAW Filters showing key Features

Not many SAW filter options exist for the UHF Amateur radio band. Both the SF0433020 and the MA09155 have much improved passband's of 22.9Mhz. However, both options were ruled out due to the operating temperature range only going down to -30C^o. While the proximity to the primary amplifier would likely prevent the filter from seeing this cold of a temperature, a wider operating temperature range is preferred. The MA09629 operates over the full temperature range from -40 to +80C^o, and a passband of 18MHz, which was the best found that still works on the Amateur Radio UHF band. An insertion loss of 2.3 dB is quite a bit on the front end, however, the uplink margin shown in Table 3 shows enough uplink margin that use of this SAW filter will not make or break the budget, while improving noise rejection. Additionally, a front end SAW filter allows for integration of a second transmitter operating on another band without saturating the Low Noise Amplifier of the UHF receiver.

6 UHF Communication System Design

6.1 Overview

Figure 6 shows the overview diagram of the new UHF Daughterboard. Since the AX5042 uses an internal transmit to receive switch, two external switches are necessary to provide the transmit and receive lines. The UPG2214TB switch was selected for its low insertion loss and small size. The SKY13299 is selected for its high power handling and switch isolation to protect the SAW filter from damage while transmitting at up to 2W. The LC LP Filter is part of the matching network for the RF5110G.

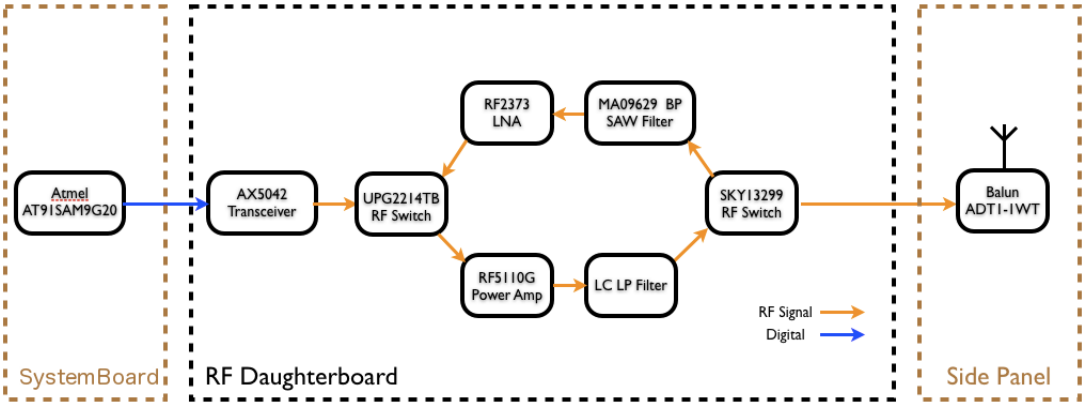

Figure 6: Overview diagram of new UHF Daughterboard

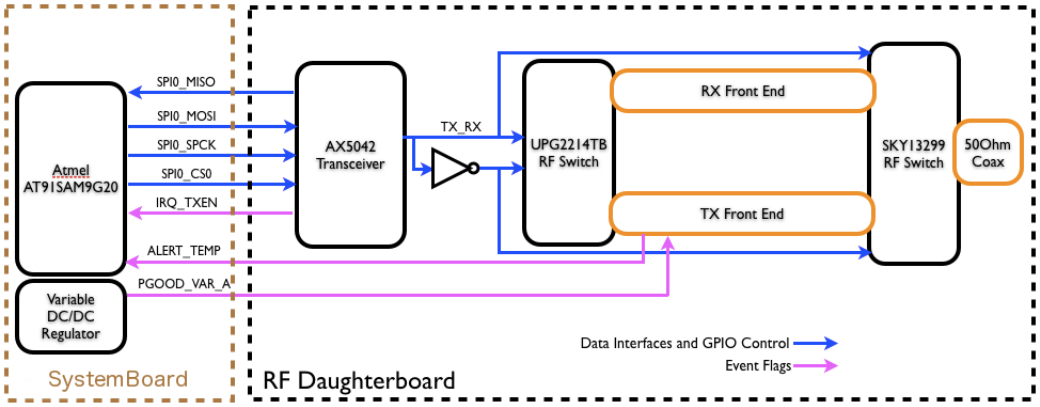

Figure 7: Overview diagram of digital interfaces and logic for new UHF Daughterboard

6.2 Schematics

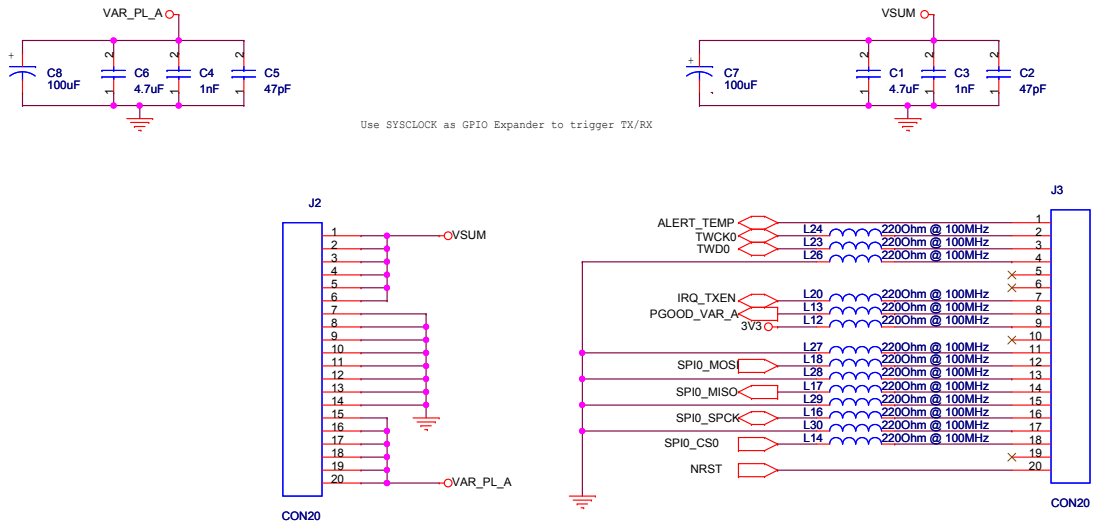

Figure 8: Page 1 of schematic showing connector interface

The first page of the schematic shows the interfaces on the daughterboard, and the filtering performed on all signals coming from the Systemboard. All the power lines have bypass capacitors of varying values to filter out noise. Additionally, all the data lines have ferrite beads in series, which at higher frequencies appear resistive. These ferrite beads were selected based on the peak operating frequency of the SPI lines expected to be 2MHz. Signal descriptions are listed below.

VSUM: Unregulated battery power. Supplies the LNA and Transceiver through dedicated low noise linear regulators.

VAR_PL_A: Regulated power that is dynamically controllable from 1.2-5.5V through resistor values on the Systemboard. This rail powers the primary RF Amplifier, and allows control of the output power by adjusting the supplying voltage.

3V3: Regulated, low power 3.3V supply used to power logic and sensors.

ALERT_TEMP: Signal generated from a temperature sensor near the RF52110G Amplifier indicating an over temperature condition. This signal both forces the RF Amp off, and the flag is available to the Atmel processor so the system software can take the fault into account.

TWCK0: I^2C line used for the temperature sensor.

TWD0: I^2C data line use for the temperature sensor.

IRQ_TXEN: Interrupt generated by the AX5042 transceiver indicating the FIFO memory within the transceiver is in a state to be read out to the Atmel processor.

PGOOD_VAR_A: Signal generated by the power regulator on the Systemboard indicating whether or not the output is within regulation. This signal will turn off the RF Amp if the the supply is not within regulation, which could occur during startup of the regulator, or in an over temperature condition on the Systemboard.

SPI0_MOSI: SPI data line to send bits from the Atmel processor to the AX5042 transceiver.

SPI0_MISO: SPI data line for the Atmel processor to receive bits from the AX5042 transceiver.

SPI0_SPCK: SPI line used to clock data too and from the Atmel processor and AX5042 transceiver.

SPI0_CS0: Select line to give the AX5042 transceiver access to the shared SPI bus.

NRST: Power-On-Reset coming from the Atmel processor. Not utilized on this board.

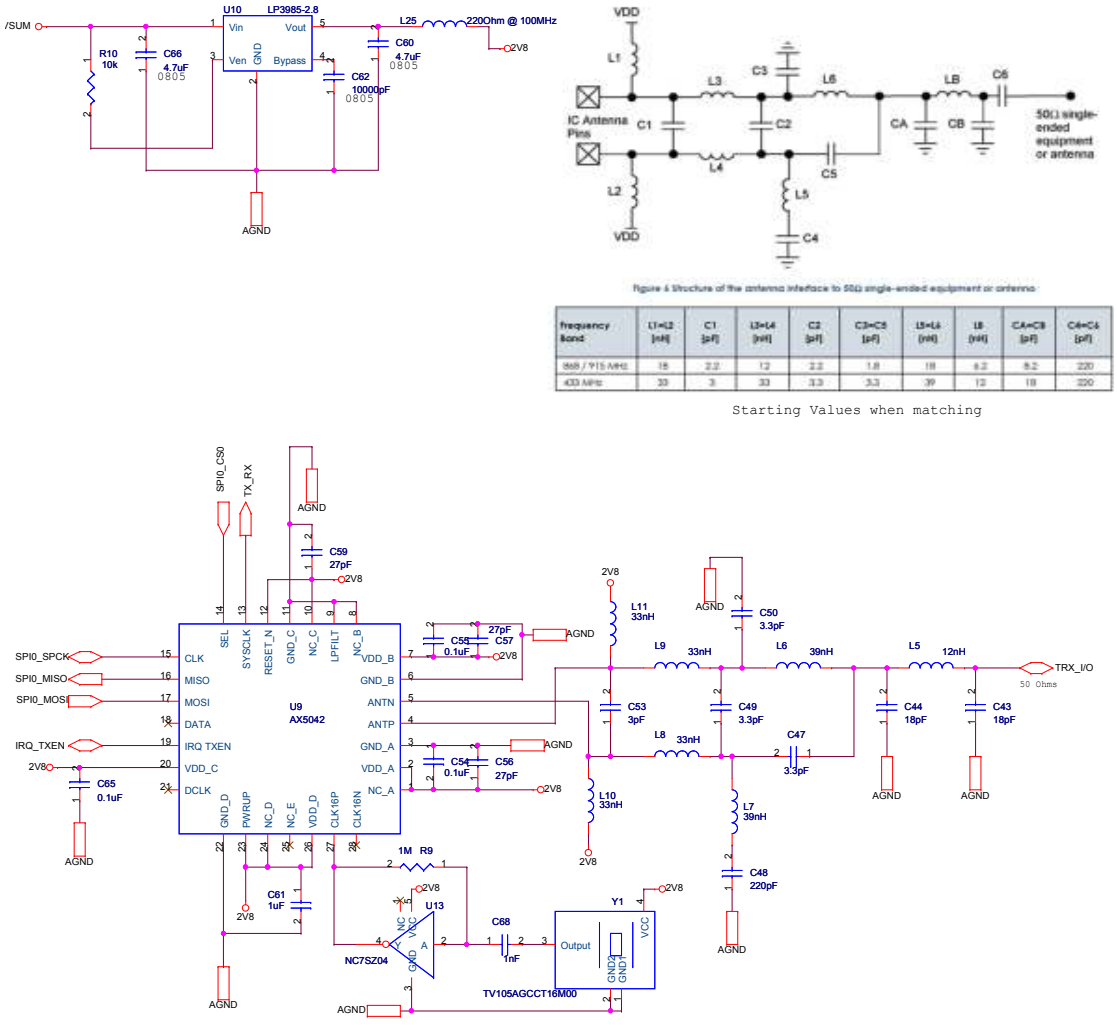

Figure 9: Page 2 of schematic showing AX5042 transceiver, crystal, power regulation, and RF matching.

The second page of the schematic shows the transceiver, its power source, matching network and crystal. The supply comes from a low noise, low dropout linear regulator (U10) providing 2.8V to the transceiver. The output of the regulator has a ferrite bead to further reduce noise, and to prevent RF signals from the AX5042 from propagating back through VSUM power rail. The recommended reference frequency is a 16Mhz clock. To reduce frequency drift on the satellite side, a Temperature Compensated Crystal Oscillator (TCXO) is selected. The buffer on the output of the crystal converts the sinusoidal signal to CMOS logic, which the AX5042 datasheet calls for. The expected stability is around 3ppm, and will age by about 2ppm one year after its manufacture date. This is a significant improvement over the previous design, removing temperature dependent frequency drift shown in Table 7 This addition, along with accurate doppler shift calculations should improve the receive

ability as the correct carrier is generated at the spacecraft for down-mixing and demodulation.

The matching network is taken from the AX5042 datasheet for a 433MHz system. It converts the balanced inputs meant for direct interfacing to a dipole antenna, to a transmission line with a 50Ω impedance. This is necessary due to the front end signal conditioning the design requires shown in Figure 6. The Pi-network made up from L5, C43, and C44 is a low pass filter to remove spurious signals.

TX_RX: Essentially an SPI controlled GPIO. This signal is the logical control for the two RF switches to place the RF front end in either receive or transmit mode. A logic HIGH is for transmit, a logic LOW is for receive.

The third page shows the RF switches used to select the transmit and receive lines. Each switch requires two GPIO inputs that must be the inverse of each other. To accomplish this, a simple logic chip inverts the TX_RX signal. Also shown is the RF 2373 LNA supplied from VSUM through a low noise linear regulator (U7) with a ferrite bead to prevent RF from electrically coupling back into the rest of the system through the power rail. This linear regulator is also controlled by the inverted TX_RX line to turn off the LNA when transmitting to both save power and protect the chip. The input and output of the LNA also contain matching networks. The MA09629 is a drop in narrowband SAW filter from Table 11 with 50Ω inputs and outputs.

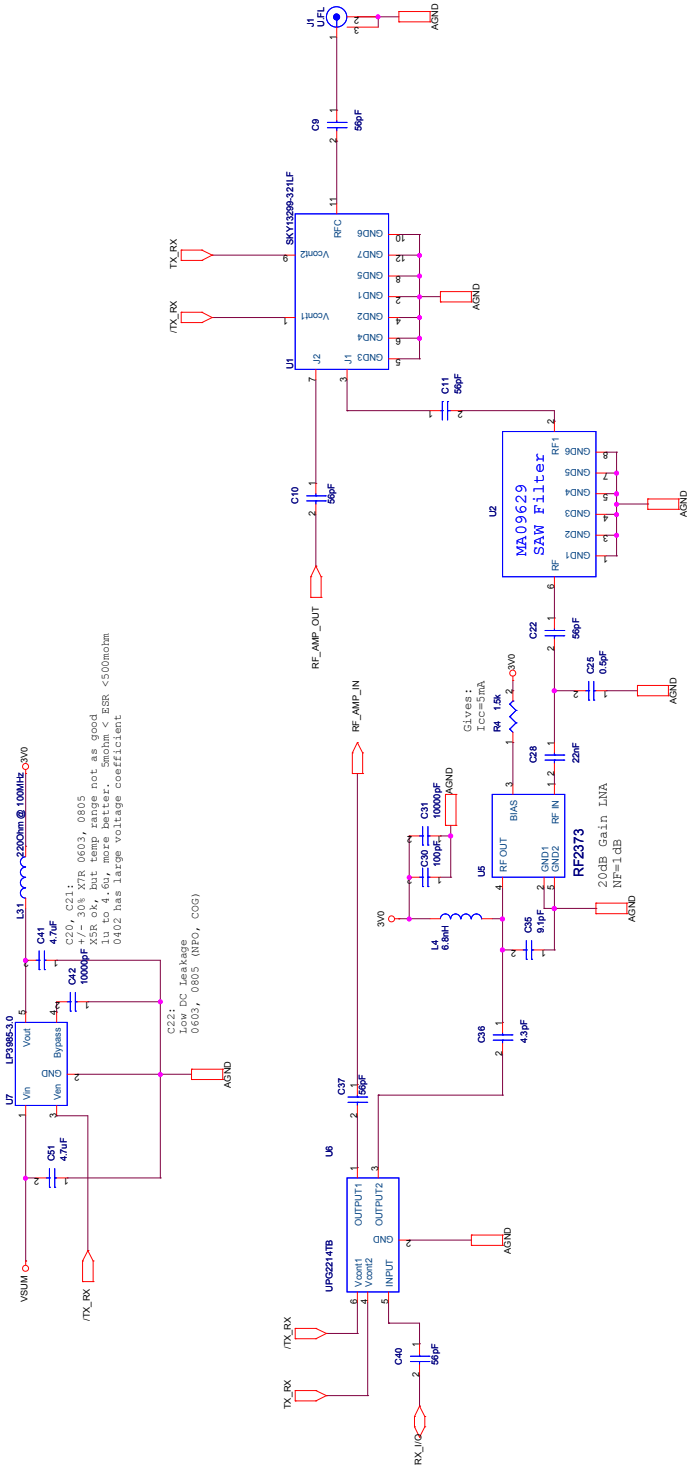

Figure 10: Page 3 of schematic showing receive chain, and transmit / receive switching

The fourth page of the schematic shows the RF5110G amplifier and it's matching network. The matching networks are taken from the reference design for 433MHz from the datasheet. The output matching network also acts as a low pass filter to reduce spurious harmonics. The inputs to the amplifier is already matched to 50Ω across the operating frequencies. The VAPC1 and VAPC2 signals can control the output power of the amplifier, with a hit to efficiency. These would typically be used when the supply voltage is allowed to vary while sampling the output RF signal. If the supply voltage rises to produce an RF signal strength that may damage the chip, the control loops acts to reduce the voltage on VAPC1 and VAPC2 to prevent damage. In this design, a control loop is not used, and the supply voltage is defined by the user, though still variable. For peak efficiency, the datasheet recommends the voltage at VAPC1 and VPAC2 to be 2.8V. When 0V, the RF5110G is powered completely off, even when the supply voltage exists. This features is used to power the RF5110G off for over-temperature conditions, if the supply voltage falls out of regulation, or if the UHF Daughterboard is set to receive mode.

A concern for the transition from transmit to receive, and receive to transmit led to having two signals control the transition from one mode to the other. If a single line is used, when going from transmit to receive, then depending on how long it takes for the RF amp to turn off, and how long it takes for the LNA to turn on, and for the RF switches to transition, could result in a scenario where the LNA is switched on, while the amplifier is still transmitting. So, in addition to the TX_RX line, the Atmel Processor must also turn on the regulator feeding the supply for the RF Amp. The timing of these events will be optimized in software to minimize the transition time and to maximize the data downlinked. For further protection against damaging the front end, even if the regulator feeding the RF Amp is not switched off prior to transition to receive mode, the TX_RX line will force the RF5110G off by a separate mechanism, though not with ideal timing. If a transient state occurs where the system broadcasts while trying to receive, the reverse isolation of the RF switches, and power handling of the SAW filter and LNA will prevent damage.

RF5110G_CTRL: Comes from the output of a 2.8V LDO (U8). When the LDO is on, the RF5110G is operating at peak efficiency, when off, the RF Amp is off.

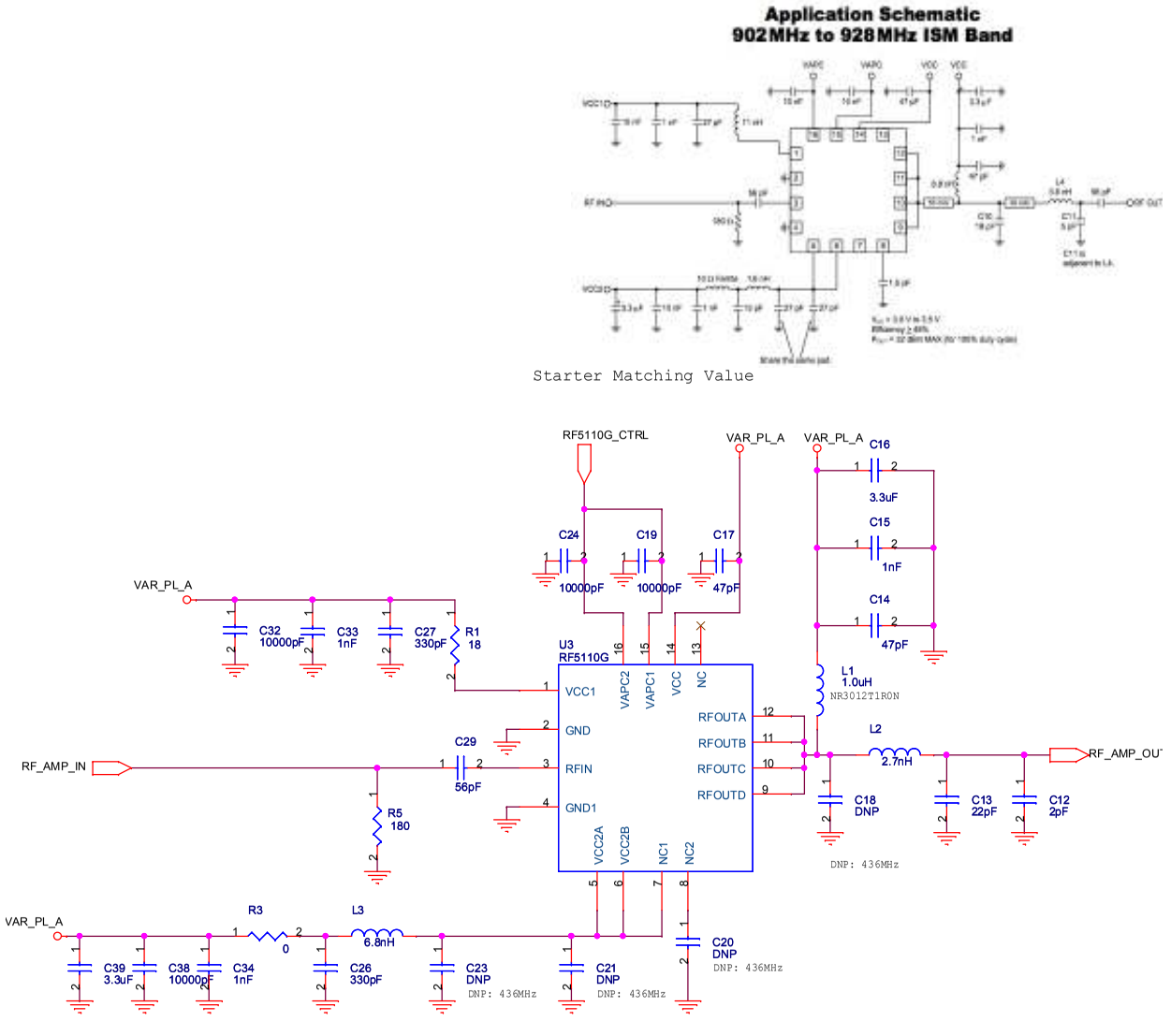

Figure 11: Page 4 of schematic showing RF5110G power amplifier with matching network

The fifth page shows some of the logic controlling the RF Amp. U4 is a temperature sensor with a programmable threshold with hysteresis that outputs and active low flag when the temperature exceeds a certain value. The PGOOD_VAR_A signal from the regulator feeding the RF Amp, along with a buffered TX_RX signal all connect to the enable pin for the linear regulator that generates the 2.8V signal that controllers whether or not the RF5110G is on. Since all these signals are open-drain, this effectively creates an OR function. In other words, if the amp overheats, or the supply voltage falls out of regulation, or the UHF Daughterboard goes into receive mode, the RF5110G is powered off when U8 is powered off.

6.3 Layout

The layout for any RF related systems is critical. At frequencies in the multiple GHz range and beyond, the layout essentially *is* the design. Since the Systemboard dimensions and interfaces were previously defined, the board size, signal pinout, and mounting holes are defined for this daughterboard. The board is only 36mm wide, and 83mm long, with the data and gpio signals originating from one side of the board, and power the other. The pins where these signals originate are shown in Figure 13d. The design uses four layers to keep down cost, with a stack up as follows:

1. Top Layer: Signal routing with controlled impedance of 50Ω to Layer 2
2. Layer 2: Ground Plane
3. Layer 3: Power and signal routing
4. Layer 4: Ground Plane with minimal signal routing.

Due to the very low stack height (1.6mm), no components are used on the bottom layer. The connection interfaces are etched pads that mate to spring loaded pins. Additionally, the bottom layer is used for routing only when absolutely necessary to minimize noise coupling from the Systemboard. The grounded vias surround the core of the elctronics in the shape of a rectangle is there to allow mounting of an RF cage over the sensitive electronics. For the RF signal to enter the cage, a microstrip to stripline transition is made through a via. All signal and power lines get filtered by capacitors and ferrite beads respectively prior to entering the RF cage. The following general layout guidelines were followed rigorously:

- Bypass capacitors as close to power pins of IC's as possible

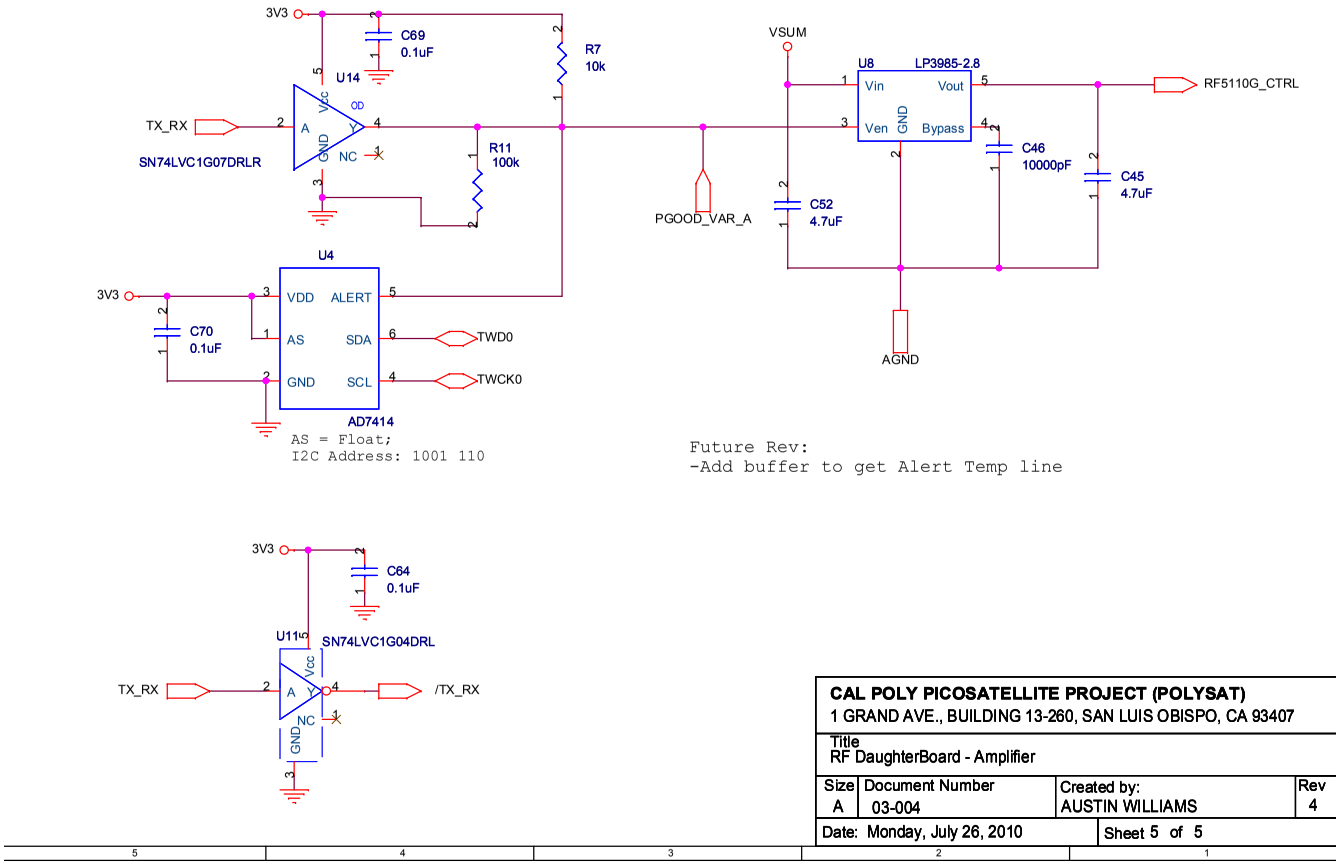

Figure 12: Page 5 of schematic showing logic for controlling the transmit receiver switching, along with a temperature sensor.

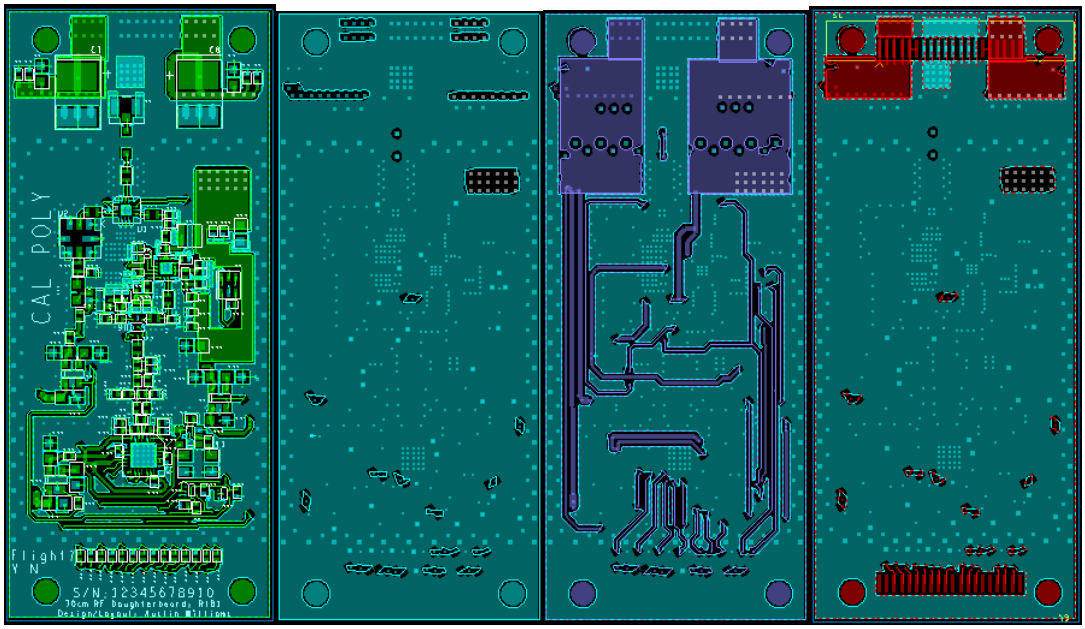

(a) Top **(b)** Layer 2 **(c)** Layer 3 **(d)** Bottom

Figure 13: Layout for the new UHF Daughterboard.

- For power lines, thick traces and a star routing configuration is used to minimize return current overlap.
- Signal on different layers route perpendicularly to each other.
- Flood ground on all layers in un-used space to ensure minimum ground impedance, minimize current loop inductance (thereby decreasing noise coupling), and maximizing thermal mass.
- Lots of grounded vias through flooded ground planes
- Lots of vias for high current power rails.
- Controlled impedance for RF lines.

By following these layout guidelines, and isolating the sensitive RF components from the rest of the system, the noise floor should be superior to the previous design. Figure 14 shows a picture of the first revision of the design. Key elements of the design are labeled with numbers shown below.

1. AX5042 Transceiver
2. Temperature Controlled Crystal Oscillator (TCXO)
3. UPG2214TB RF Switch

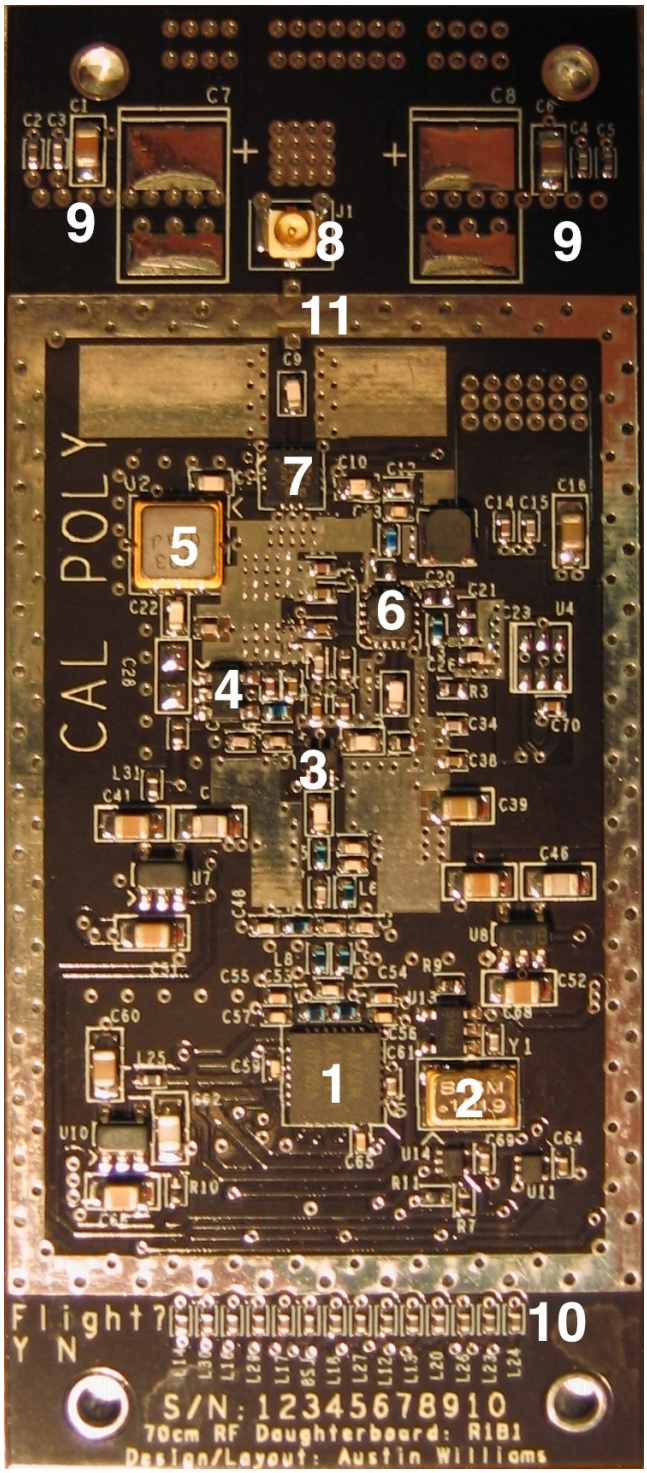

Figure 14: Pictures of the Rev 1 UHF Daughterboard.

4. RF2373 Low Noise Amplifier

5. MA09629 SAW Filter

6. RF5110G RF Amplifier
7. SKY13299 RF Switch
8. U.FL 50Ω Connector
9. Capacitors for smoothing out power rails
10. Row of ferrite beads filtering all data and gpio lines
11. Exposed ground with via's for installment of custom RF cage

7 Impedance Matching and Component Performance

7.1 Low Noise Amplifier Impedance Matching

The 2373DS Low Noise Amplifier will provide a low noise figure on the front end to improve the receive sensitivity of the receiver. According to RF Micro Devices, the front end of the LNA is broadband matched to optimize the noise figure, and the input does not require tuning. The output tuning will set the forward gain.

7.1.1 S-Parameters for Low Noise Amplifier

Component footprints C36 and C35 from Figure 16 provide an L matching network for the device. Two coax leads are tapped into the RF chain by removing C22 and U6. Both these locations present a 50 ohm load under normal operations due to the SAW filter and switch. The outer shielding of the coax is first grounded to the board, and then zip ties restrain the coax from moving, shown in Figure 17. Prior to soldering the center conductor to the RF chain, each coax is connected to a calibrated two port Network Analyzer. The Network Analyzer reference place is then manually shifted until the S11 and S22 smith charts show an open circuit. The shift in reference plane for the coax at the input and output represents the electrical length of the coax, and ensure the reference plan is positioned at the solder point on the RF chain.

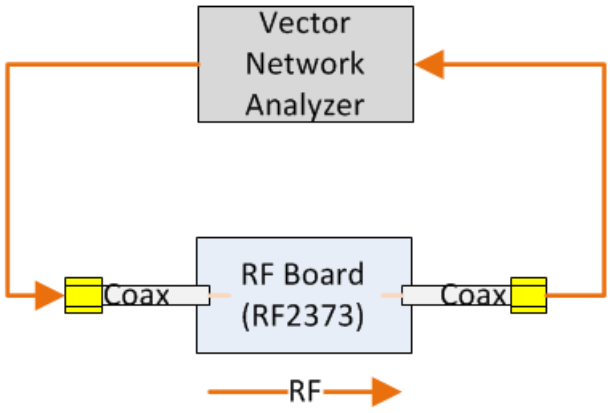

Figure 15: Diagram showing the test setup to measure the LNA S-Parameters

The initial S-Parameter measurements are shown in Figure 18. Not much attention was payed to the input matching of the LNA initially, as RFMD indicated that it should not require tuning provided the datasheet was followed. The output matching will set the forward gain (S21) at our target

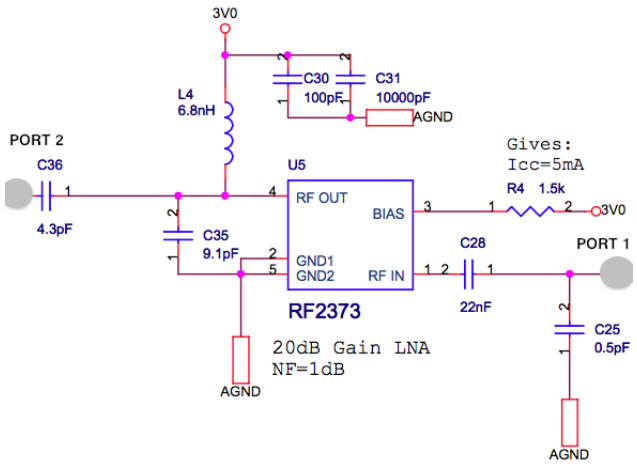

Figure 16: 2373DS Circuit with initial matching network

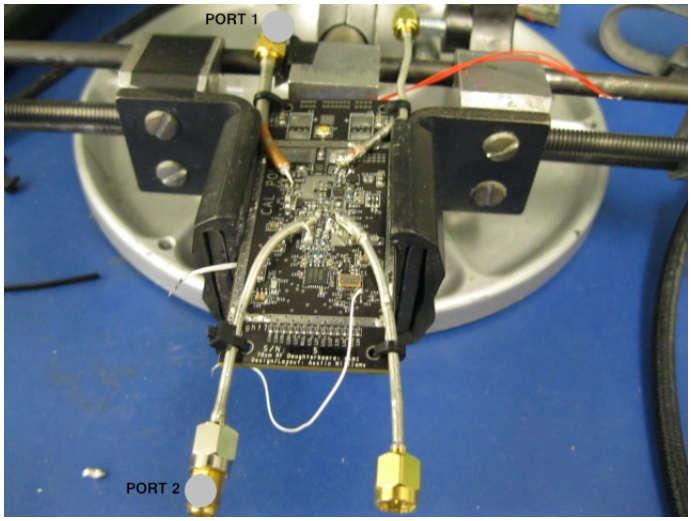

Figure 17: RF Board showing two coax lines taped at the input and output of the LNA

frequency of 437Mhz. The output is clearly not matched well, providing a forward gain of only 14.6dB, and a return loss of only -3.63dB. The initial parameters tuned the board nicely for around 500 Mhz, but this is outside the desired operating range of the system.

To begin matching port 2, the following process was used:

1. Connect port 2 directly to the output of the IC by removing C36, and shorting across it with a 0 ohm resistor.

2. Remove C35

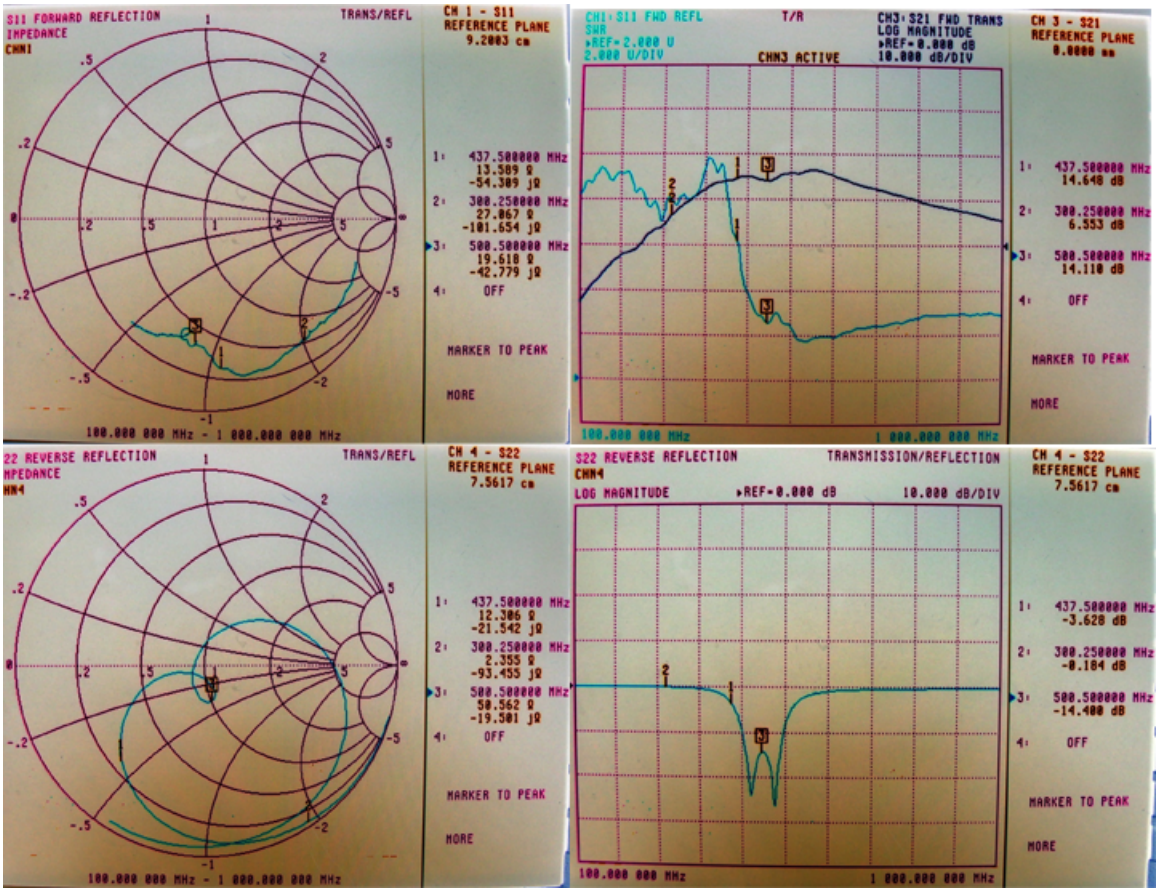

Figure 18: Initial S-Parameter measurements using initial matching values from 100Mhz to 1Ghz. **TopLeft:** S11 measurement for input of the LNA broadband matches for noise figure. **TopRight:** S21 forward gain measurement showing peak gain of 14dB, well below the specification in the data sheet of 23 dB. **BottomLeft:** The S22 measurement showing a good match around 500 Mhz with a measured impedance of 50.56 - j10.5 Ohms. **BottomRight:** A magnitude plot of the S22 measurement showing a return loss of -14dB at 500Mhz, and -3.6dB at 437Mhz.

3. Take an S-Parameter measurement to get a good approximate value for the impedance presented by the output of the LNA

4. Using a Smith Chart, plot the impedance point, and design a first cut L matching network to transform the impedance to 50 ohms.

5. Solder the calculated C35 value, and take another S-Parameter measurement to verify it's movement along the smith chart.

6. Adjust the value slightly above or below the previously test value to fine tune the transformation to get as close to the desired location as possible.

7. Remove the C36 short, and solder the previously calculated value.

8. Fine tune the value slightly above or below the previously tested value to approach a good 50 ohm match.

An assumption being made here is that the distance from the reference point at the tip of the coax conductor, to the IC, is insignificant. This is a valid assumption given the extremely tight layout, and and the large wavelength of the frequency used (approximately 70cm). A useful rule of thumb is if the length is less than 1/20th of the wavelength (3.5cm), than that trace length does not need to be treated as a transmission line. Additionally, any error introduced by this assumption is compensated for by fine tuning with inductor or capacitor values around the calculated value. The final matching values are showing in Table 12, with S-Parameter measurements show in Figure 19.

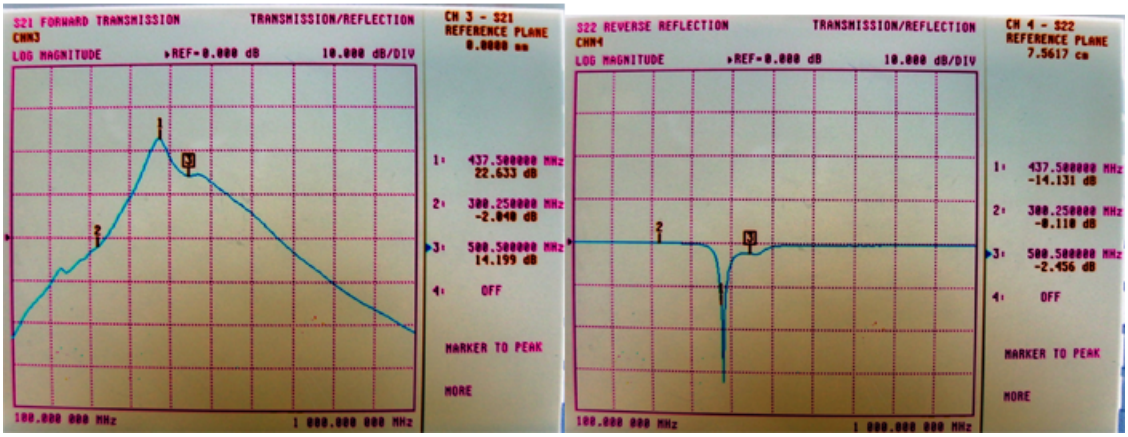

Figure 19: S-Parameter measurements using final matching values measured from 100Mhz to 1Ghz. **Left:** S21 measurement showing a forward gain of the LNA of 22 dB at 437Mhz, well in line with datasheet expectations. **Right:** S22 measurement showing the return loss at 437Mhz is -14dB, indicating a good match.

MatchingNetwork	C35Value	C36Value	ForwardGain	ReturnLoss
Initial	9.1pF	4.3pF	14.3dB	-3.63dB
Final Matching	12pF	2.7pF	22.6dB	-14.1dB

Table 12: Improvement in forward gain from proper matching

7.1.2 Noise Figure of Low Noise Amplifier

The front end noise figure with the final matching values from Table 12 were measured. Since my experience with taking noise figure measurements is very limited, I want to ensure the test setup is valid. To demonstrate the test setup, the RF2373 evaluation board is measured, which has a known noise figure. A picture of the test setup is shown in Figure 20. An external noise source (Agilent

n962) is used. The ENR table is provided on a floppy drive and loaded into the Network Analyzer as part of the calibration process. The Noise Figure is a 1 port measurement, where the external noise source is powered from the back of the Network Analyzer, and fed to the input of the LNA, with the output attached to port 1. Figure 22 shows a screen capture for the measured noise figure of the LNA evaluation board. Table 13 shows the comparison between the expected datasheet value for the noise figure, and the measured noise figure. The values coincide, so measurements on the custom hardware can be taken with confidence.

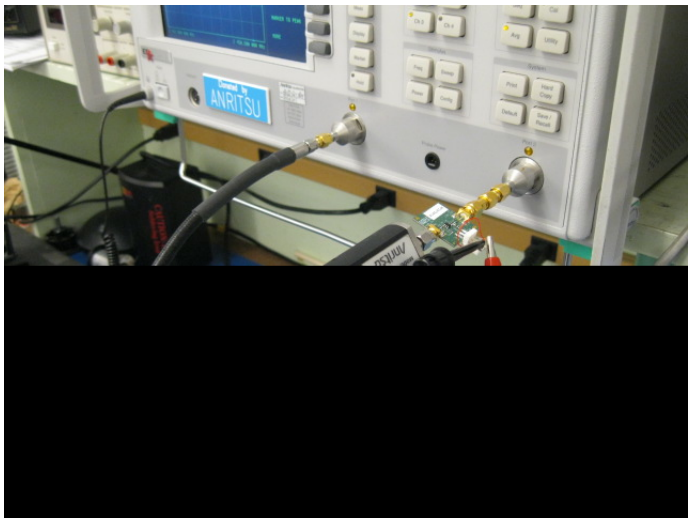

Figure 20: Picture of the Noise Figure test setup using the RF2373 Evaluation Board at 2.45Ghz measuring a noise figure of 1.362dB The datasheet states a noise figure between 1.3dB and 1.5dB.

Figure 21: Diagram showing the test setup to measure the Noise Figure

The settings for the Noise Figure measurements for the evaluation board are shown below:

- Fc = 2.45Ghz

The initial S-Parameters shown in Figure 28 show that, similar to the LNA, the component is tuned too high. A nice match for 527Mhz is there, but needs to work at 437Mhz. The S11 return loss is around -10dB from about 200Mhz to greater than 1Ghz, which shows the good broadband input match. The same process was used as the LNA to generate good matching values at the output. The final matching circuit is shown in Figure 29, where L2 is replaced with 3.6nH, and C13 is replaced with 27pF. It was ultimately found that adjusting capacitor values C20 and C21 for second stage tuning had very little impact on the match, or the efficiency, so they were left at there default values. A small signal gain of around 33dB was expected, and ultimately achieved.

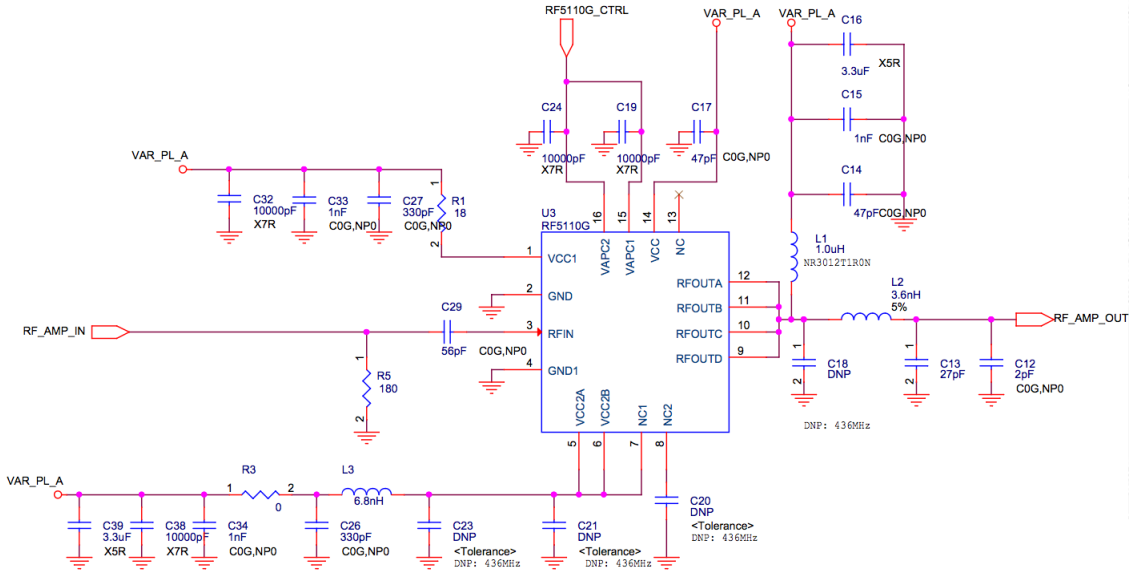

Figure 29: Final matching network for the RF5110G

Figure 30: Final S-Parameter measurements for the RF5110G from 100Mhz to 1Ghz. **TopLeft:** S11 impedance measurements showing a match of 51.1 -j3.2 Ohms at 437Mhz. **TopRight:** S21 forward gain measurement of 33.1dB. The data sheet specifies a forward gain of 33dB. **BottomLeft:** S22 return loss of -31dB at 437Mhz, showing a good match.

7.2.2 Efficiency of RF Amplifier

A very nice feature of the heritage Cal Poly UHF System using the now obsolete RF2117 amplifier was powering it directly off the unregulated battery voltage. This leads to a slight variation in transmit power depending on the state of charge of the battery, but resulted in a very efficient system since no power regulation was required, which usually takes a 10 to 15% efficiency hit. The RF5110G output power is very sensitive to variations in supply voltage, and will typically be operated at voltages below 3.3V. The high variability in transmit power vs supply voltage is exploited to allow tuning of output power for a given mission requirement.

A variety of tests were performed with the RF5110G under various operating conditions to determine the efficiency. An HP436A Power Meter is used with an HP8481A Power Sensor. The sensor can handle a peak continuous input power of 300mW, which means attenuation is required during the measurements. The same coax taps used for the RF amplifier tuning is used for the power

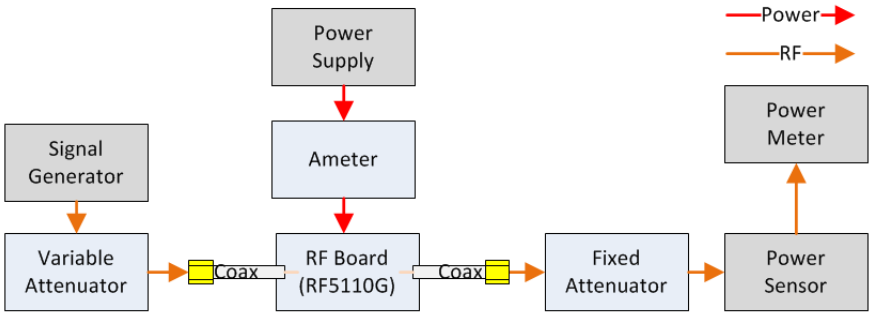

Figure 31: Diagram showing the test setup to measure the RF Amplifier efficiency

efficiency measurement. The test setup uses a signal generator to produce a 100% duty cycle CW 437Mhz signal at a variety of input RF drive strengths between -2dBm to +10dBm. For an accurate measurement of the efficiencies, it's important to have an accurate measure of the RF Output power, which the Power Meter provides, along with accurate knowledge of DC power to the Amp. A DC power supply allowed voltage control to the supply of the amp, and a digital multimeter provided current readings. Additionally, I^2R losses are taken into account in the long power and ground cables coming from the power supply. The resistance of the cables was measured, and found to be approximate 0.13 Ohms. Ultimately the efficiency of the amplifier is calculated using the following equation:

$$\frac{P_{RFOut}}{(I_{RFSupply} * V_{RFSupply}) - P_{LineLoss}} * 100 = \eta_{Amp} \tag{3}$$

Prior to performing the measurements, the user manual for the HP436A was found online, and a calibration procedure performed to ensure the device is providing valid readings.

The expected efficiency for the amplifier at 450Mhz is 50.5%. Figure 32 shows the custom, matched amplifier operating at a variety of supply voltages and input RF powers. It's pretty clear that the RF drive power has a minimal impact on the output RF power. Lower RF drive powers tend to be slightly less efficient, but not by much. With efficiencies approaching 50%, the device is operating very nearly to specification according to the data sheet. The high operating efficiency also validates the decision to leave the second stage matching of pins 5 and 6 at their default settings.

Vcc (V)	Rfin (dBm)	Current (mA)	RF Out (mWatts)	Wire Loss (mW)	Adj Eff (%)
3.6	10	1382	2339	248	**49.5**
	8	1384	2355	249	**49.8**
	6	1375	2323	246	**49.4**
	4	1362	2296	241	**49.3**
	2	1346	2244	236	**48.7**
	0	1310	2148	223	**47.8**
	-2	1255	1977	205	**45.8**
3.4	10	1305	2089	221	**49.6**
	8	1305	2089	221	**49.6**
	6	1302	2080	220	**49.4**
	4	1293	2065	217	**49.4**
	2	1282	2032	214	**49.0**
	0	1258	1968	206	**48.3**
	-2	1208	1828	190	**46.7**
3.2	10	1230	1858	197	**49.7**
	8	1224	1841	195	**49.5**
	6	1226	1849	195	**49.6**
	4	1222	1841	194	**49.5**
	2	1211	1811	191	**49.2**
	0	1196	1770	186	**48.6**
	-2	1153	1660	173	**47.2**
3	10	1153	1633	173	**49.7**
	8	1150	1626	172	**49.6**
	6	1151	1629	172	**49.7**
	4	1148	1618	171	**49.4**
	2	1143	1611	170	**49.4**
	0	1129	1574	166	**48.9**
	-2	1097	1489	156	**47.5**
2.8	10	1073	1419	150	**49.7**
	8	1068	1403	148	**49.4**
	6	1073	1419	150	**49.7**
	4	1070	1413	149	**49.6**
	2	1065	1400	147	**49.4**
	0	1061	1387	146	**49.1**
	-2	1038	1324	140	**47.9**
2.6	10	992	1222	128	**49.8**
	8	986	1199	126	**49.2**
	6	990	1216	127	**49.7**
	4	992	1219	128	**49.7**
	2	986	1205	126	**49.4**
	0	981	1191	125	**49.1**
	-2	971	1156	123	**48.1**
2.4	10	914	1038	109	**49.8**
	8	909	1026	107	**49.4**
	6	910	1028	108	**49.5**
	4	909	1026	107	**49.4**
	2	909	1028	107	**49.6**
	0	909	1023	107	**49.3**
	-2	899	995	105	**48.5**
2.2	10	831	859	90	**49.4**
	8	826	849	89	**49.1**
	6	829	855	89	**49.3**
	4	829	855	89	**49.3**
	2	829	853	89	**49.2**
	0	824	839	88	**48.7**
	-2	823	836	88	**48.5**
2	10	745	693	72	**48.9**
1.8	10	665	552	57	**48.4**
1.6	10	579	421	44	**47.7**
1.4	10	476	290	29	**45.6**
1.2	10	318	135	13	**36.7**

Figure 32: Efficiency of the matched RF5110G using different supply voltages and RF drive levels. The efficiency is constant to within a few percentage points across voltage and drive levels until really low voltage supplies.

7.2.3 Spurious Harmonics of RF Amplifier

An important performance parameter for the system is the strength of out of band spurious noise from harmonics of the transmit frequency. The matching network taken from the RF5110G evaluation boards states the matching network also provides a low pass filter functionality. Trying to find a spurious out of band power requirement was not terribly straight forward. Starting with the Amateur Radio Regulations [12] in Part 97 of the FCC regulations, there is a brief discussion of Emission Standards under Subpart D §97.307.

1. §97.307(c) - Blanket statement saying all emissions from a station transmitter must be reduced to the greatest extent possible.

2. §97.307(d) - Under 30Mhz transmitters require the mean power be 43dBc below the fundamental emission.

3. §97.307(e) - Transmitters between 30MHz and 225Mhz, and transmitting below 25W must keep harmonic spurs below 25uW and at least 40dBc below the fundamental emission, but need not be reduced below 10uW.

Emission standards for the 70cm Amateur band are not directly addressed, and thus fall under §97.307(c), requiring a best effort. A useful datapoint is the out of band emissions for an iCom-910H, which is the current radio used at PolySat's ground station, and a popular radio in the community. According the the iCom-910H [13] brochure, the transceiver has spurious emissions less than -60dBc for the 430MHz band, and is capable of transmitting between 5 to 75W.

Figure 33 shows the initial performance with the current matching network and filtering. The board is set to transmit around 1W of RF power through several attenuators, directly into the spectrum analyzer. The initial performance is poor, with a large $2F_o$ spur of -24.4dBc, and a smaller $3F_o$ spur of -41.1dBc.

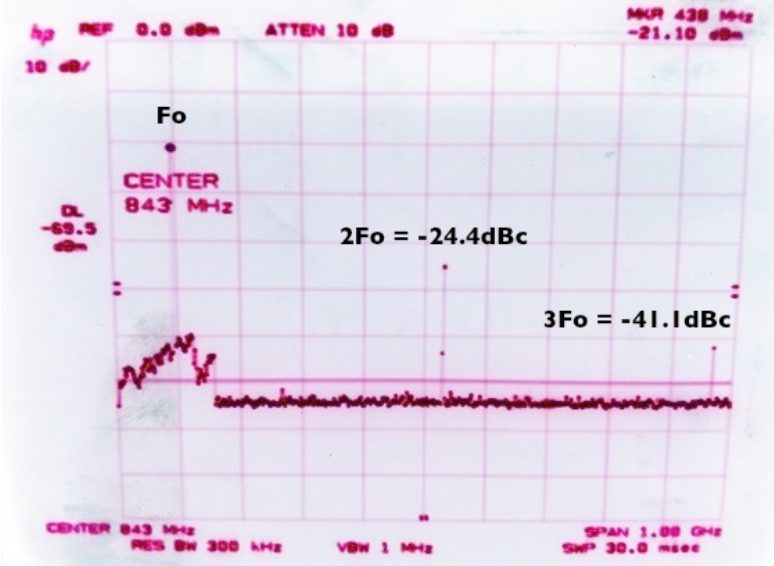

Figure 33: Snapshot of the initial spurs seen. The $2F_o$ spur is at -24.4dBc, and the $3F_o$ spur is at -41.1dBc.

Fortunately, there is a footprint for a capacitor C20 designed onto the board that is initially left as a Do Not Populate based on the 450MHz reference design for the RF5110G amplifier. This footprint connects directly to the output of the chip at the gold wire bond. Using the inductance of the gold wire bond plus surrounding parasitic inductances in combination with a shunt capacitor allows for resonant tuning to the $2F_o$ frequency, creating an effective RF short at that particular frequency, which will notch out the spur.

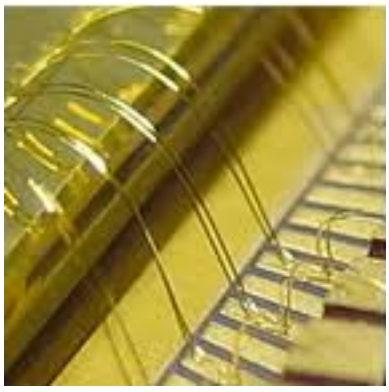

Figure 34: Image of gold wire bonds. An external capacitor resonating with the gold wire inductance is used to filter out the $2F_o$ frequency.

The capacitor value needs to be found experimentally since the actual inductance is heavily dependent on the layout. The first value tried was 8.2pF based on other values used on the RF5110G

reference design, and it completely notched out the $3F_o$ spur, which likely meant it was resonant at that frequency, and would allow me to calculate the effective inductance. By definition, at resonance the reactive portions of the impedances are equal and opposite, as shown in Equation 6

$$2\pi fl = \frac{1}{2\pi fc} \tag{4}$$

Letting $f = 3F_o = 1311Mhz$, and $c = 8.2pF$, solve for inductance l

$$l = \frac{1}{(8.2 * 10^{-12})(2\pi * 1311 * 10^6)^2} = 1.8nH \tag{5}$$

Having an approximate effective inductance we can now find the capacitance that provides resonance at $2F_o = 874Mhz$

$$c = \frac{1}{(1.8 * 10^{-9})(2\pi * 874 * 10^6)^2} = 20pF \tag{6}$$

So, I would expect to see resonance somewhere around 20pF. Table 15 below confirms this, where at 18pF, the best attenuation of $2F_o$ is seen. Unfortunately, this should have been done as part of the matching process, since adding this capacitor did slightly change the matching network, as the transmit power had dropped by around 1dB. This meant the matching network required tweaking to account for the added shunt capacitance to the line. It was experimentally found that changing the output series inductor L2 from 3.6nH to 3.3nH, and the output shunt capacitor C13 from 27pF to 22pF returned the amplifier to optimal transmit powers, and also reduced the spurious noise. Lastly, a simple 3rd order filter from Coilcraft was placed in series with the coax with a -3dB cutoff frequency of 700Mhz to further reduce spurious noise. The $2F_o$ spur was further reduced to -56dBc, while the $3F_o$ spur was pushed below the noise floor of the spectrum analyzer at the resolution bandwidth used.

Configuration	**$2F_o$** (dBc)	**$3F_o$** (dBc)
Initial: C20 = DNP	24.4	41.1
C20 = 8.2pF	-29.1	-56
C20 = 15pF	-37.1	-49.2
C20 = 18pF	-41.3	-48.4
C20 = 22pF	-35.9	-51.2
C20 = 18pF, L2 = 3.3nH, C13 = 22pF	-49	-51.5
C20 = 18pF, L2 = 3.3nH, C13 = 22pF, LPF	-56	–

Table 15: Summary of $2F_o$ resonance tuning.

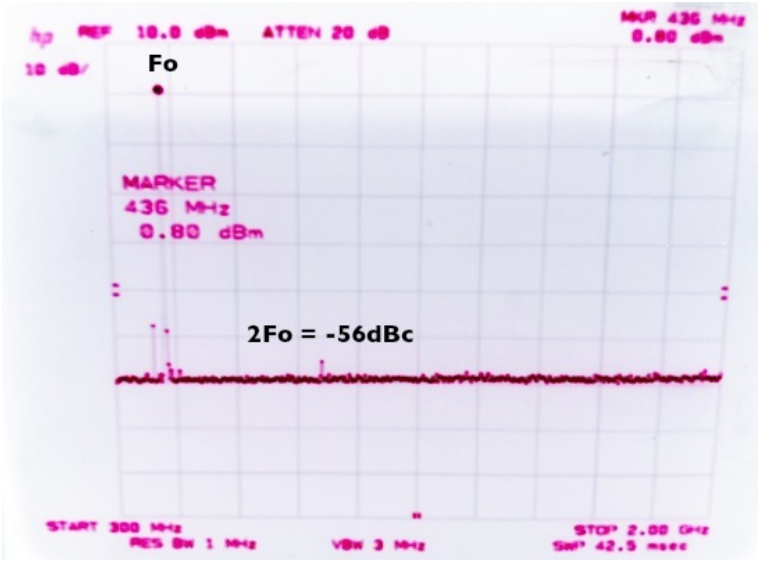

Figure 35: Snapshot of the final spurs seen after final tuning and addition of 3rd Order LPF on the output to remove higher order harmonics. The $2F_o$ spur is at -56dBc, and the $3F_o$ spur is below the noise floor with the RBW set to 1Mhz, and a span of 2GHz.

Figure 35 shows the final broadband transmit spectrum, and elimination of spurs. Assuming a maximum transmit power of 2W, a spur 56dB down is approximately $5\mu W$. The most stringent emission requirements come from §97.307(e), which requires harmonics to be kept below $25\mu W$, but need not be reduced below $10\mu W$. Given that these requirements are exceeded, use of this transmitter on amateur radio bands will not cause harmful out of band interference.

8 System Performance

Since a large component of a fully functional system is the transceiver driver, full system testing could not be completed until a functional driver was written for the UHF System, and integrated into the Linux operating system. This software was written in parallel with the hardware design by members of the PolySat software team, with huge contributions from Dr. Bellardo, a Computer Science faculty member. Prior to testing the fully integrated system, a method to measure the receive sensitivity of both the Axsem transceiver evaluation board, and the custom RF Board was developed to obtain performance numbers with known functional software. After completion of the transceiver driver and the supporting Linux process for packet generation and RF Board hardware control, system level testing took place to characterize the overall performance.

8.1 Receive Sensitivity

The Axsem transceiver evaluation board includes a USB module with an 8051 micro-controller flashed with firmware to control an AX5042 transceiver that is plugged into the USB module. By using two modules, generic test packets are easily generated, and bounced between one another, while allowing control over Frequency, Data Rate, Modulation Scheme, Modulation Index, Test Packet Size, and crystal value. To provide a baseline comparison, the sensitivity of the Axsem evaluation board is measured based on the test setup shown in Figure 36. Two 8051 micro-controller boards interface to a PC via two USB connections. One module is kept outside of the faraday cage, and acts as the transmitter. It transmits through a variable attenuator, providing attenuation in 1dB increments, and through a 3dB splitter, which routes the signal to the device under test housed inside the faraday cage, and also to a spectrum analyzer with a low noise amplifier on the front end. The low noise amplifier lowers the noise floor of the spectrum analyzer, allowing for measurements of signals below -120dBm. The faraday cage needs to only provide enough isolation between the transmitter and receiver so stray RF emanating from the board doesn't bypass the RF coax. This is verified by simply cranking up the attenuation to see the device under test stops receiving packets. If packet reception continues, than the test setup has no control over the RF level reaching the receiver.

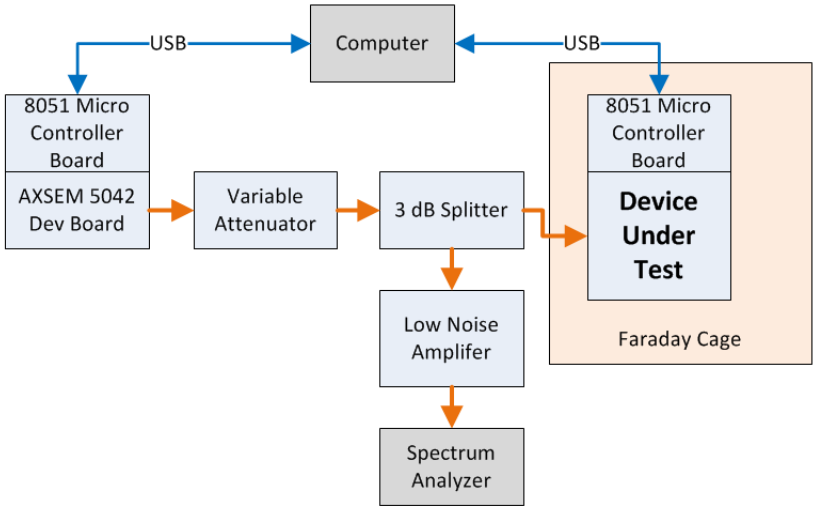

Figure 36: Test setup used to measure the receive sensitivity of the Axsem 5042 evaluation board, and the custom made RF Board.

The results of the Axsem evaluation board sensitivity is shown in Figure 37 for various data rates and modulation schemes. The number of packets transmitted, and the drop rate are also included. Already, these results are a dramatic improvement over CP3, CP4, and CP6. At 1.2kbps FSK, the transceiver drops no packets at -113dBm, and has a drop rate below 1% at -114dBm, and which close to the -115dBm sensitivity of the current ground station. Given the ground systems reliable reception of much weaker signals originating from around 0.5 to 1W of RF power coming from the CubeSats dipole antenna, results comparable to the current ground station are very encouraging as we can confidently say the link will close as the ground amplifier of 100W will provide significant margin.

DataRate (kbps)	Modulaton Type	Packet Length (Bytes)	# Packets Transmitted	Packet Error Rate (%)	Signal Strength (dBm)
1.2	FSK	8	504	0	-113
			505	0.4	-114
			505	3.6	-115
			613	21	-116
2.4	FSK	8	505	0.8	-114
			508	5.7	-115
4.6	FSK	256	680	0.1	-110
			500	0.2	-111
			561	3.2	-112
		8	1004	1	-113
			525	7.8	-114
9.6	FSK	256	1000	0	-93
			1000	0	-103
			1000	0	-106
			1000	0	-108
			1022	1.37	-110
		8	1008	0.1	-110
			1005	0.8	-111
			1010	3.4	-112
			1004	10	-113
19.2	FSK	256	1003	0	-104
			1003	0	-106
			1003	1.5	-108
38.4	FSK	256	1006	0.4	-105
	PSK	256	1005	0.2	-106
			1007	0	-107
			1009	0.1	-108
			1008	0.5	-109
			1007	3	-110
100	FSK	256	1014	0	-97
			1013	0.5	-99
	PSK	256	1020	0.4	-102
			1013	0.8	-104
			1231	2	-106

Figure 37: Sensitivty of the Axsem evaluation Board for various data rates, packet sizes and modulation schemes

A similar test is performed using the custom RF Board, running the same software. This allows for direct comparison of hardware performance with the evaluation kit. An improvement over the evaluation kit performance is expected from the low noise amplifier on the front end of the transceiver on the RF Board. It's not clear how much of a performance gain is expected due to the front end SAW filter, which has an insertion loss of around 2dB. A lot of consideration went into the order of the LNA and SAW filter. Ultimately, having the SAW filter in front of the LNA protects the LNA from saturation from another transmitter either external or internal to the satellite. Given the expected performance of the radio to close the link with significant margin, it was ultimately decided that eliminating the potential of LNA saturation from out of band transmissions is worth while. Figure 38 shows the tabulated results. As expected, the custom RF Board outperforms the Axsem evaluation board by around 6dB. At 1.2kbps, the RF Board drops no packets at signals down

to -119dBm. This is an improvement over CP3/CP4 and CP6 of around 27dB and 19dB respectively. While encouraging, these numbers represent an ideal environment since the faraday cage shields outside noise, and the measurements do not account for potential self jamming caused by the Systemboard running Linux, which contains several high frequency components. The final system performance is characterized with a similar measurement technique, though performed as a long range test in a more real world environment.

DataRate (kbps)	Modulaton Type	Packet Length (Bytes)	# Packets Transmitted	Packet Error Rate (%)	Signal Strength (dBm)
1.2	FSK	8	613	0	-119
			519	0.2	-120
			508	0.8	-121
			545	6.3	-121
2.4	FSK	8	555	0	-118
			541	0	-119
			543	0	-119
			509	0.4	-120
			524	1	-121
			594	5	-121
4.6	FSK	256	222	0	-115
			206	0	-117
			313	0.6	-118
			315	9.2	-119
		8	585	0.2	-118
			509	0.8	-119
			524	3.2	-120
			371	14.5	-121
9.6	FSK	256	534	0	-97
			506	0	-107
			553	0	-111
			510	0	-114
			502	0	-116
			503	4	-117
		8	508	0.2	-117
			510	1.5	-118
19.2	FSK	256	511	0	-108
			557	0	-111
			747	0	-112
			561	0.2	-114
			514	0.4	-115
			516	3.1	-116
38.4	FSK	256	575	0	-109
			527	0	-112
			550	0.5	-113
			522	5.5	-114
	PSK	256	592	0	-112
			596	0	-114
			542	0	-114
			532	0	-116
			534	1.1	-116
			517	7	-117
100	FSK	256	1023	0	-101
			1147	0	-104
			1037	0.4	-106
			1236	1.2	-107
	PSK	256	1115	0.7	-107
			1028	1	-108
			1102	1.5	-109
			1058	1.2	-110
			1029	0.9	-111
			1022	1.9	-112
			1080	4.4	-113

Figure 38: Sensitivity of the RF Board for various data rates, packet sizes and modulation schemes showing the improved performance on the custom board compared the results from the evaluation board shown in Figure 37. The improvement is due to the Low Noise Amplifier added to the front end of the receiver.

8.2 Design Issue: Blown Amplifier

With known functional hardware, the next step was mating the custom RF Board to the Systemboard, running PolySat's software for the first time. This allows for complete testing of the system since the sensitivity testing performed in Section 8.1 manually set the transmit / receive switches to either transmit, or receive. The design allowed for independent control over both the RF Amplifier enable line, and the RF switches incase timing issues occurred. Including this feature turned out to be critically important, as the first RF Board interfaced with the Systemboard running our own software could send and receive packets, however the amp was immediately blown. The software sequence was carefully stepped through, and a potential issue was found. When the board goes from transmit to receive mode, the amp is turned off by disabling a DC/DC switching regulator on the Systemboard. The PGOOD_VAR_A signal, and the removal of V_{CC} to the RF Amp both turn off the device. At the same instant the DC/DC switching regulator is powered off, the RF Switches are set to receive mode. The issue, is that the RF Switches can switch on the order of nano-seconds, while the amp takes several milli-seconds to power down. As a result, while the Amp is still partially powered, an open circuit at the switch exists, showing up as a very poorly matched load at the RF Amp output terminal, causing large power reflections and ultimately damaging the device. Figure 39 shows an oscilloscope capture of the gradual power down of V_{CC} going to the RF5110G amplifier. Channel 1 is V_{CC}, and Channel 2 shows the TX_RX signal that controls the RF Switches. The RF Switches transition almost instantly, while the amplifier power gradually decays.

Figure 39: CH1: RF5110G V_{CC} Supply from switching regulator on Systemboard. CH2: TX_RX signal controlling the RF Switches. 100μs per division.

The gradual decay of V_{CC} is not an issue provided V_{APC} powers down immediately. Figure 40 shows that this is not the case. Channel 1 is again V_{CC} for the Amplifier, while Channel 2 is the V_{APC} signal, which originates from the linear regulator U8. Both signals take much longer than

10ms to fully discharge. The solution to the problem is to add pull-down resistance to the output of U8 to significantly reduce the turn-off time, and include a software delay between turning off the switching regulator powering the RF Amp, and the signal that switches the board from transmit to receive mode. The simplest solution is to add a very long delay, but doing so causes a significant hit to the actual data through-put since a delay on the order of 100ms is required, and occurs every time the board transitions from transmit to receive. The Linux operating system will perform far more back and forth communication during file transfers than previous CP satellites, so a 100ms delay is not ideal. Figure 41 shows the final modification, where a 200Ω pull down resistor on the output of U8 is added. The scope capture shows the V_{APC} powering down after about 2ms. A software delay of 10ms in software is included. After adding the strong pull down resistor, and adding a software delay, the amplifiers were no longer damaged.

Figure 40: CH1: RF5110G V_{CC} Supply from switching regulator on Systemboard. CH2: V_{APC} signal providing a second mechanism to power down the amplifier. 2ms per division.

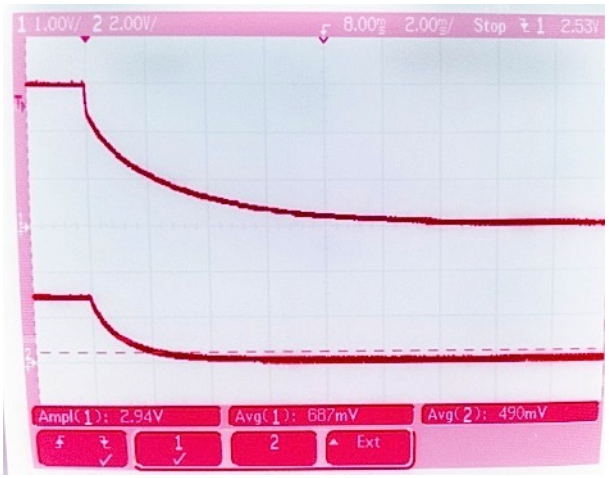

Figure 41: CH1: RF5110G V_{CC} Supply from switching regulator on Systemboard. CH2: V_{APC} signal with 200Ω pull down resistor on the output of U8. 2ms per division.

8.3 Crystal Tuning

The crystal value is a very important parameter for low data rates since, according to the data sheet, the Axsem transceiver is capable of auto-tuning to the carrier frequency within a bandwidth that is a function of the data rate. For Phase Shift Keying (PSK), the bandwidth is shown in equation 7, and for all other modulation schemes equation 8.

$$BW_{PSKAUTOTUNE} = \pm\left(\frac{DataRate}{4}\right) \tag{7}$$

$$BW_{AUTOTUNE} = \pm\left(\frac{DataRate}{2}\right) \tag{8}$$

For large data rates, crystal accuracy is not terribly important, but for low data rates, the crystal accuracy is extremely important. A significant change from the heritage Cal Poly design is the move to a Temperature Compensated Crystal Oscillator (TCXO). The TCXO generally performs with an order of magnitude improvement in stability, on the order of 3ppm, whereas cheaper crystals operate with stabilities around 30ppm. The importance of crystal tuning was made evident early in the process of playing with the evaluation boards as getting the boards to communicate at 1200bps required careful tuning of the crystal using a spectrum analyzer since the 16Mhz crystal is not actually 16Mhz. The small deviation can translate to potentially significant frequency offsets when mixed up to the 437Mhz range.

8.3.1 Tuning Process

The recommended process for tuning the crystal is to use the SYS_CLK line on the Axsem to provide a square wave out that is an integer fraction of the crystral value of 16Mhz. However, the custom RF Board is unable to do that, as the SYS_CLK line is configured by the software to act as a general purpose IO to control the RF Switches into either transmit or receive mode. A spectrum analyzer works fine for tuning as well provided the software has a CW mode. While the CC1000 has an On-Off Keying (OOK) mode for simple CW generation, the Axsem does not. We found through testing the evaluation boards that setting the modulation index to 0 for an FSK signal affectively produces a CW signal. The Modulation Index (h) is defined by Equation 9, where R is the data rate, and $f_{deviation}$ is the frequency shift from the carrier used to represent either a logic 1, or logic 0.

$$h = \frac{f_{deviation}}{R} \tag{9}$$

By setting h to 0, a pseudo-random sequence of bits will produce a CW as no frequency shift occurs. With a known good CW signal, the following procedure is used to measure the actual crystal value, and calibrate it.

1. Connect an antenna to both the RF Board and the Spectrum Analyzer
2. Start with an assumed crystal value of 16Mhz
3. Configure the Spectrum Analyzer to have a wide span (500kHz or so) so the CW signal is clearly visible
4. Gradually zoom in on the signal by reducing the span, and increasing the resolution bandwidth. Using the peak hold feature makes it easier to track the CW signal as it transmits with a 50% duty cycle.
5. Final settings for the Spectrum Analyzer are: Resolution Bandwidth (RBW) = 10Hz, Video Bandwidth (VBW) = 30Hz, Span = 100Hz, 1dB/div
6. With the above settings, let the Spectrum Analyzer sit in peak hold mode to let it trace the signal clearly on the screen. Record the approximate center of the peak.
7. The adjusted crystal value is calculated with an equation provided in the Axsem data sheet used to determine register values to set the carrier frequency in software. First, the decimal

value for the FREQ register is calculated using Equation 10 with the assumed carrier frequency in Hz, and a crystal value of 16,000,000 Hz.

$$FREQ = \left[\frac{f_{CARRIER}}{f_{XTAL}} 2^{24} + \frac{1}{2} \right] \tag{10}$$

8. Next, Equation 10 is re-arranged solving for f_{XTAL}, as shown in Equation 11. Instead of using the assumed carrier frequency, the actual measured carrier frequency is used. Since both the actual carrier are known, along with the FREQ decimal value programmed into the registers used to obtain the actual carrier, the correct crystal value is easily solved for.

$$f_{XTAL\ CORRECT} = \left[\frac{f_{CARRIER\ ACTUAL}}{FREQ - \frac{1}{2}} \right] 2^{24} \tag{11}$$

9. Set the software driver to use the new crystal frequency value, and repeat the process to verify the center frequency is correct. The crystal accuracy is dependent on the data rate used, and must account for crystal drift with temperature. This drift is discussed in Section 8.3.2, but for a 9600bps signal, a carrier accuracy within 100Hz is more than sufficient, and easily achievable as a general rule of thumb.

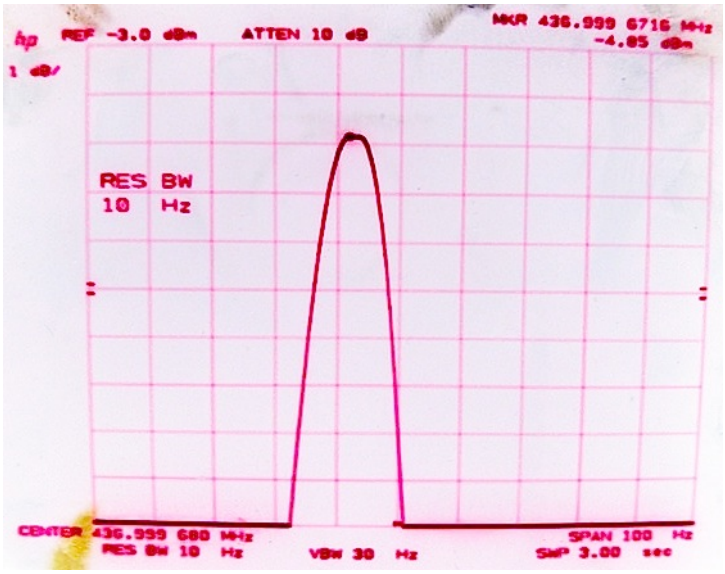

Figure 42: Pre-tuned CW with a default crystal setting of 16 Mhz, and a carrier frequency of 437 Mhz, showing an actual carrier of 436.999672 Mhz, or an error of 327Hz.

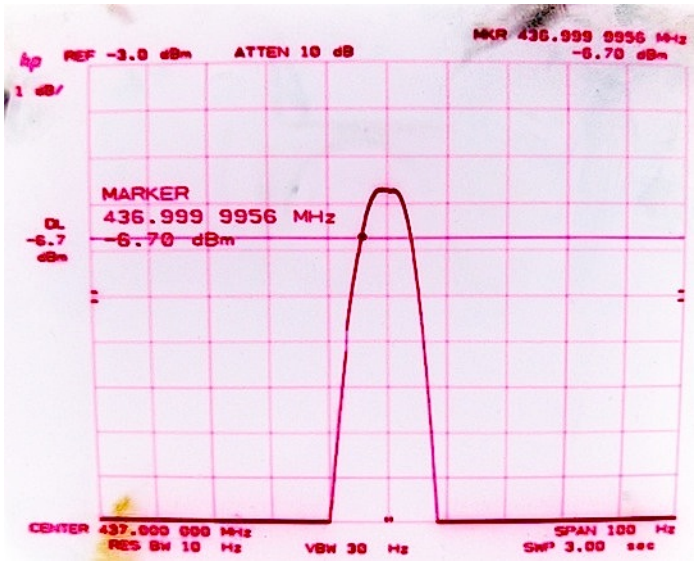

Figure 43: Post tuned CW, with a new crystal setting of 15.999988 Mhz, and an actual CW centered right at 437 Mhz.

Figure 42 shows the CW signal with a carrier frequency set to 437MHz, and a default crystal value of 16Mhz. The carrier is off by about 327Hz. Figure 43 shows the tuned CW, centered right at 437Mhz.

8.3.2 Temperature Drift

Crystal frequency values will drift with temperature. For this reason, a temperature compensated crystal was chosen. While they draw more power (around 10mW) and are more expensive than standard crystal oscillators, the benefits of tighter frequency tolerance is well worth it since low data rate uplinks are expected to ensure significant uplink margin. To get a sense of the expected shift, a simple test is performed. The board was first cooled using a compressed air can to get as cold as we could on the bench. The temperature sensor built into the board was used to read the temperature value. At +5C, the board is commanded to transmit a CW signal at 1W of RF out, with the spectrum analyzer setup with an antenna with peak hold enabled to monitor the drift over temperature. The result is shown in Figure 44, which shows a span of 1kHz, and a total drift of less than 600Hz.

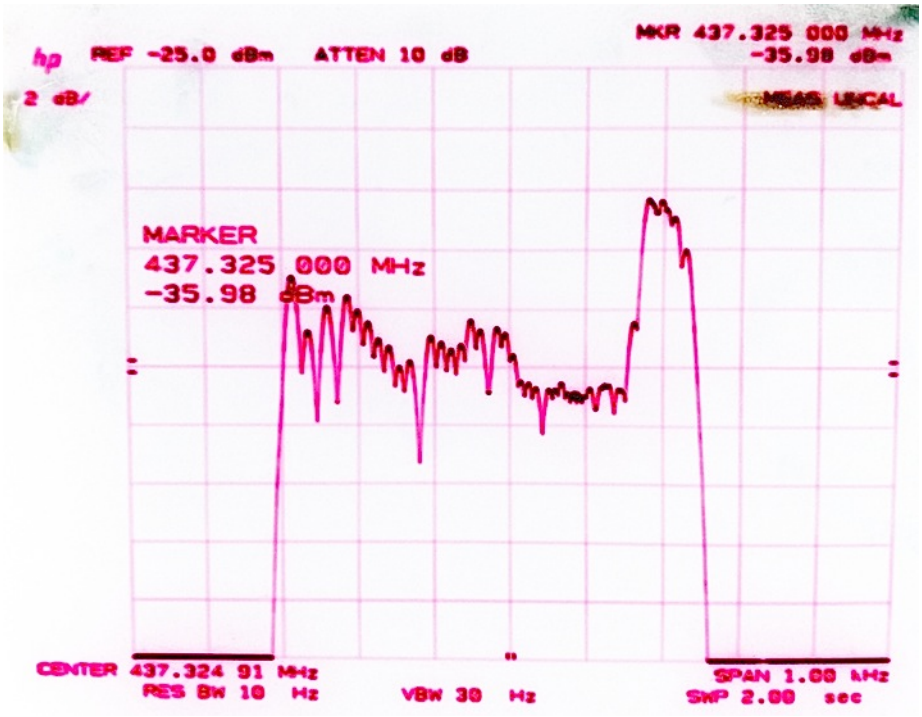

Figure 44: Frequency drift from +5C to +60C showing a drift of less than 600Hz. Spectrum Analyzer shows a span of 1kHz. The Max Hold feature of the spectrum analyzer was used to capture the drift over temperature.

It was noted that the frequency would increase with temperature consistently until around 50C, where no increase in frequency was seen between 50C and 60C. The board temperature leveled off around 60C after 30 minutes of transmission. Given a 9600bps signal properly centered around its carrier, the signal cannot drift by more than 4600Hz above or below the carrier for proper operation. This test shows significant margin over temperature to ensure reliable signal lock at our minimum desired frequency of 9600bps assuming sufficient doppler shift control at the ground station. Higher data rates become even less of an issue.

8.4 Long Range Test 1

Several long range tests were performed to obtain real world performance characteristics. The faraday cage test setups are good for determining any self jamming, but don't account for any type of antenna performance, or affects of ambient noise. The first test was performed in Shell Beach, with one person on the roof of a house, and another at the parking lot to Pirates Cove, giving a transmission distance of 4.73km with pretty good line of site. A diagram of the setup is shown in Figure 45, and is similar to the faraday cage test. The primary difference is the coax cable is replaced

by two antennas. The TX side is a Linux Systemboard and UHF Daughterboard combination, and is set to periodically beacon a packet with sensor readings, which are decoded at the receive end. The spectrum analyzer is used to read off the received power levels.

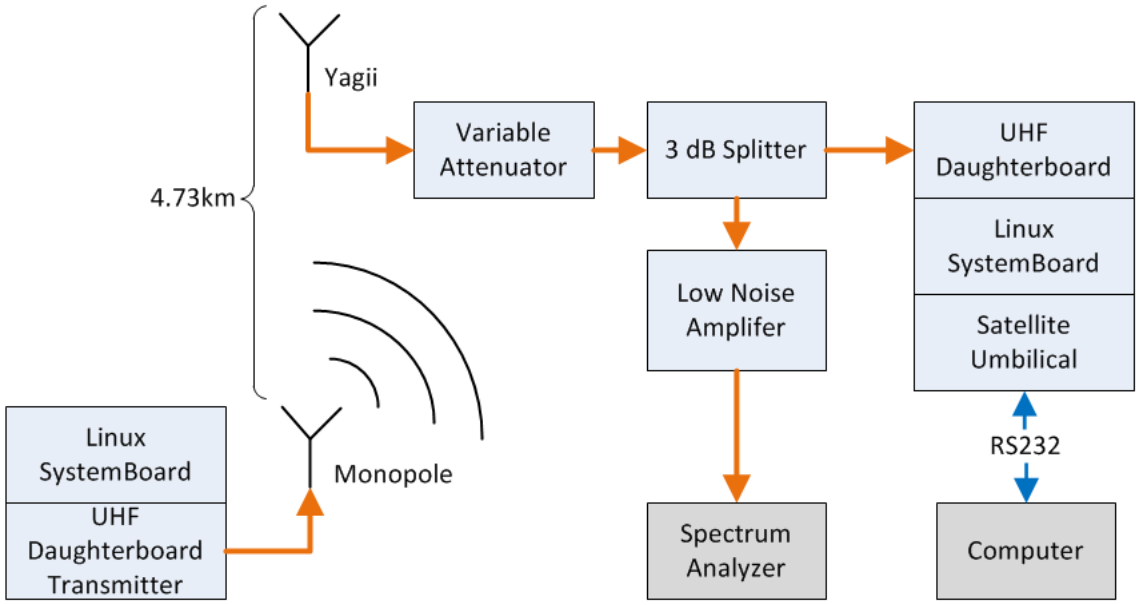

Figure 45: Test setup for the long range test used to verify final system performance. Each end of the link uses a UHF Daughterboard with Systemboard combo, at a distance of 4.7km from each other. The received signal strength is measured with a Spectrum Analyzer as the transmitter beacons autonomously once every 30 seconds.

Figure 46: Picture of the receive end of the long range test setup. The Yagii antenna is mounted to the upside down table on the left, and oriented to ensure the polarity of each antenna align since neither are circularly polarized.

$\mathbf{VariableAttenuator(dB)}$	$\mathbf{RXPower(dBm)}$	$\mathbf{DropRate(\%)}$
0	-75.9	0
30	-105.2	0
35	-109.3	0
42	-116	10

Table 16: Long Range Test 1: Monopole side set to periodically beacon a packet periodically after boot-up. Data Rate 9600bps using GMSK.

Table 16 shows that the side with the yagii and variable attenuator receives within a few dB of its ideal, indoor performance. This performance is very encouraging, as it's comparable to the performance obtained with the current Yaesu ground station, according to Ivan's Thesis [2], which states a sensitivity of around -116 dBm.

8.5 Long Range Test 2

A second long range test was performed as part of a ballon launch for our CP8 satellite, which is currently using the new UHF system for both the satellite comm link, and as a ground station. For this test, one team was setup on the roof of the Advanced Technology Laboratory, and another team sent with the hardware intended to go on the balloon launch up to the side of Bishops Peak, where a clear line of site is provided. A diagram of the test setup is shown in Figure 47. The balloon unit

uses a custom made monopole antenna, while the ground station side again used a hand held yagii, with a variable attenuator in line. The goal of the test was to approximate the receive performance of both the balloon hardware, and the ground station side, and see that they perform roughly the same. The power regulators on the ground station Systemboard were also turned on, and sourcing a large amount of current to load resistors so see if any additional noise was added to the system that impacts performance. This would be important to know for completely integrated systems.

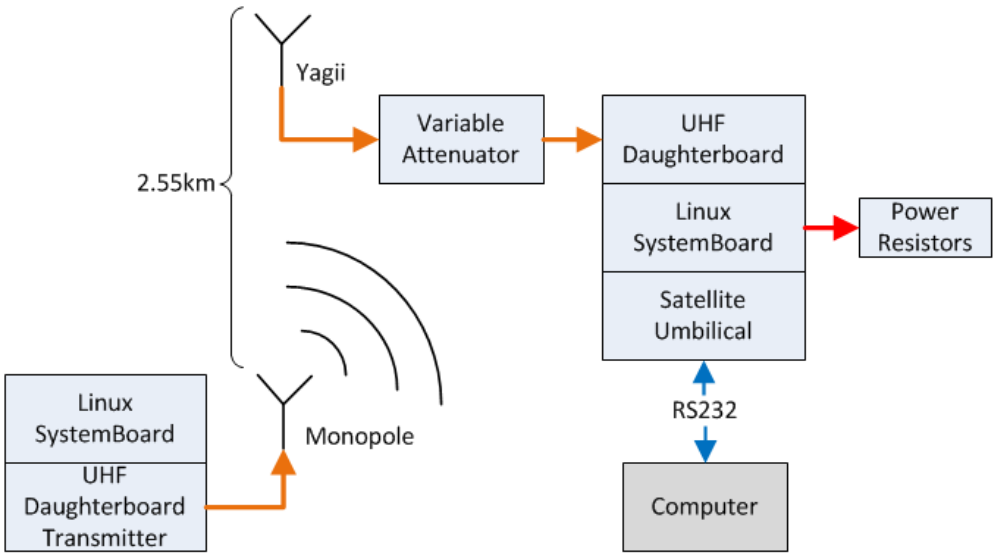

Figure 47: Diagram of setup for Long Range Test 2.

The beginning of the test is similar to test one, where the Monopole side periodically beacons upon power on, and the variable attenuator is adjusted until a cut-off point is found. After the cut-off point is found, two of the on-board regulators are turned on. One regulator provides 5.0V, and another 3.3V, each attached to a 3Ω resistor, which gives a total regulated output power of approximately 12W.

VariableAttenuator(dB)	**Regulators?**	**DropRate(%)**
40	Off	0
50	Off	0
54	Off	20
54	On	20

Table 17: Long Range Test 2: Monopole side set to periodically beacon a packet periodically after boot-up. Data Rate 9600bps using GMSK.

Table 17 shows the results of receiving on the Yagii side. Finding a variable attenuator threshold of 54dB, and turning on the regulators had no noticeable affect on the receive sensitivity. This is very

encouraging, since it shows the core satellite hardware does not self jam, or increase the noise floor, even when sourcing large amount of power from noisy switching regulators. This can be attributed to a very well thought out, and clean layout with careful placement of noisy components relative to the battery terminal.

Next, the yagii side was configured to ”ping” the monopole side. This is a ping in the same sense of two networked computers pinging each other. One computer sends a packet to the other, which receives it, and responds with a packet of its own, displaying the round trip time. For a ping to be successful, both sides must properly receive and transmit. To ensure each side is as similar as possible, the transmit powers are made as identical as reasonably possible, so approximate performance information can be extracted from the variable attenuator setting. If the sides have the same receive capability, and the same transmit power, a ping should be reliable at very close to the same variable attenuator setting due to antenna reciprocity.

$\mathbf{VariableAttenuator(dB)}$	$\mathbf{Regulators?}$	$\mathbf{DropRate(\%)}$
0	Off	0
10	Off	0
20	Off	2
25	Off	25

Table 18: Long Range Test 2: Initiating a Ping command from the Yagii side. Data Rate 9600bps using GMSK.

Table 18 shows the results, where the side with the monopole is dramatically less sensitive than the yagii side. The difference from the previous test is roughly 30dB. Having the balloon capable of receiving the entire time was not a requirement, and did not hold up that particularly project, though the design of that antenna appears to have a very high noise temperature. Another antenna test was planned for after the balloon flight to debug this issue. Figure 48 shows an image take with the balloon unit from Bishops during the test. The Ground side commanded the balloon unit to take the images, which were then downlinked over the UHF System using an FTP protocol. This was the last demonstration performed during the test, and showed considerable functionality. Prior to downlinking the image, the ground system SSH’d into the balloon unit’s Linux computer, and changed the data rate from 9.6kbps to 100kbps to demonstrate we have remote data rate agility, and also to reduce the time it took to downlink the image. Figure 49 shows an image taken by the same balloon unit during the actual launch. None of the recovered images were actually downlinked due to data rate limitations, and because were were trying to recover thousands of images. All the pictures were pulled from an SD Card after recovery, but all beacons were received on the ground

station side, and most of the time, the ground station was telnetting into the balloon units Linux computer over the UHF link. Again, the downlink was more reliable than the uplink, which we anticipated.

Figure 48: Image from the Long Range Test 2. The Yagii side commanded the Monopole side (Balloon Unit) to take several pictures. This image was then downlinked over the UHF link. It also demonstrated a neat capability, where the yagii side SSH'd into the Balloon Unit over the UHF link, and changed the data rate from 9.6kbps, to 100kbps for the image downlink.

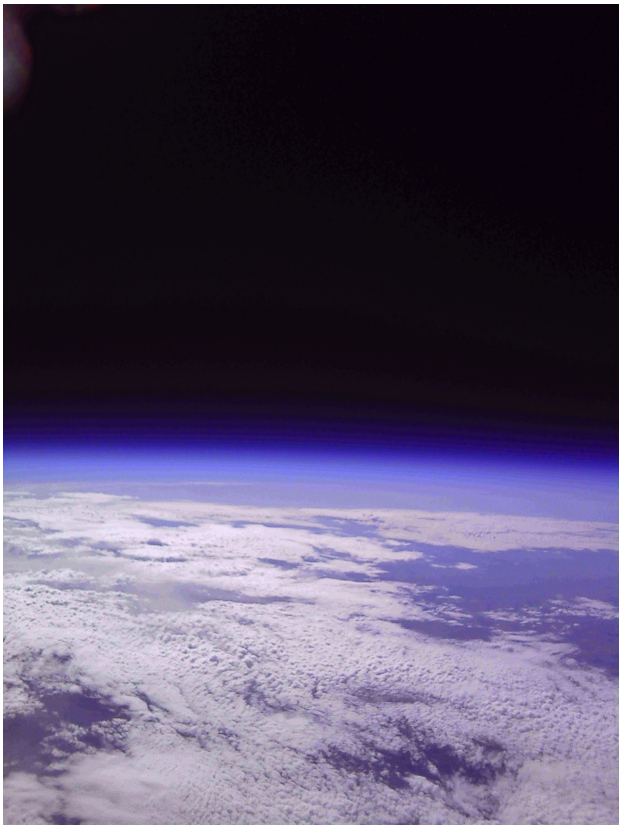

Figure 49: Image taken during the balloon launch. For the duration of the launch, the ground side received all beacons. The ground side was also telnetting into the Linux computer over the UHF link for control. Eventually, uplink was very inconsistent, which was expected given the results of Long Range Test 2. All images from the actual launch were recovered on an SD card due to data rate limitations.

8.6 Long Range Test 3

We wanted to re-create the long range tests in a lab like environment, where swapping out parts, and changing configurations would be convenient. We also wanted to use two matching, yagii antenna's to rule out a poor antenna design. Figure 50 shows the initial test setup, where the receiving side with the Spectrum Analyzer was in one lab, while the transmitter was in an adjacent building. The transmissions would go through the walls. Additionally, a single computer would locally control the receiver, and SSH over the school network into the transmitter. This allowed for a terminal window for each Linux system to be viewed side be side. The transmitting side used a custom application that allowed for a single packet to be transmitted, and the receiving end would indicate whether or not a packet was received.

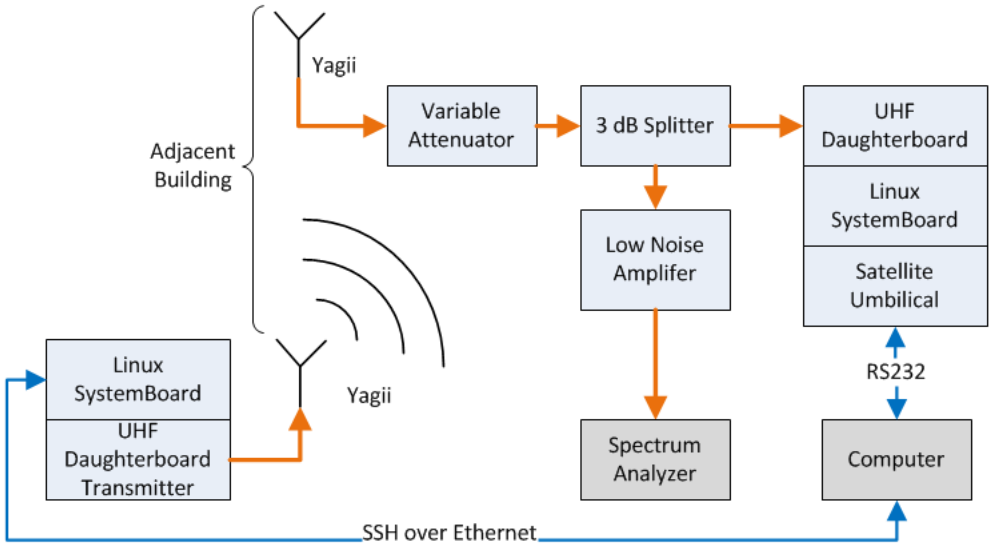

Figure 50: Initial setup for indoor Long Range Test. Now, two matching Yagii's are used.

Additionally , a better procedure for measuring the signal strength was developed due to the variability in transmit power from transmission to transmission likely since the transmissions were going through walls. The transmit power was kept low, around 100mW for safety reasons. The procedure used is outline below:

1. Build the test setup according to Figure 50.
2. For a data rate of 9.6kbps, set the Spectrum Analyzer Span to 50kHz
3. Set Resolution Bandwidth to 10kHz, to approximately match the AX5042 digital filter
4. Set the scale to 2dB/Div
5. Set the reference level for the scale according to the signal strength so the transmission is seen on the screen
6. Press Max Hold
7. Send a packet
8. Press Peak Search, record the power, and whether or not the packet was received.
9. Press, clear, then repeat from step 6.

Using the above process provided far more accurate results since every packet sent has its received power accurately measured. The edge of packet loss is very clear, to where one can use just

the spectrum analyzer reading, and know whether or not the packet went through with high precision. The sensitivities shown are the apparent thresholds, as opposed to averaging a large number of packets.

Config	Description	Sensitivity(dBm)
A	Initial setup, shown in Figure 50	-113
B	Setup A, with Systemboard and UHF Stack Swapped	-114
C	Setup from Figure 51, Attenuation on TX	-104
D	Setup C, with Systemboard and UHF Stack Swapped	-104
E	Setup from Figure 52, Attenuation on TX, 20dB on RX	-114

Table 19: Long Range Test 3: Indoor testing. Data Rate 9600bps using GMSK.

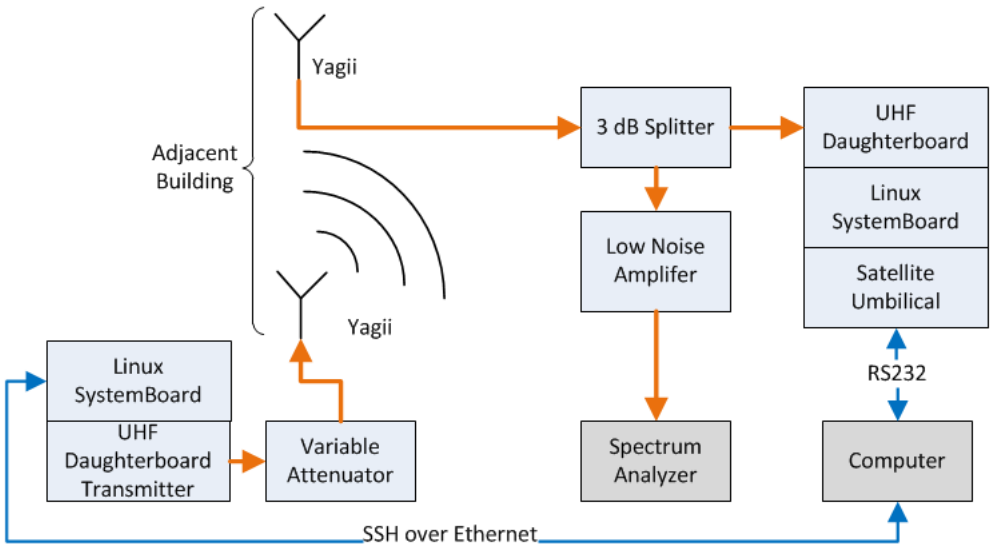

Figure 51: Indoor test setup with the variable attenuation moved to the TX side.

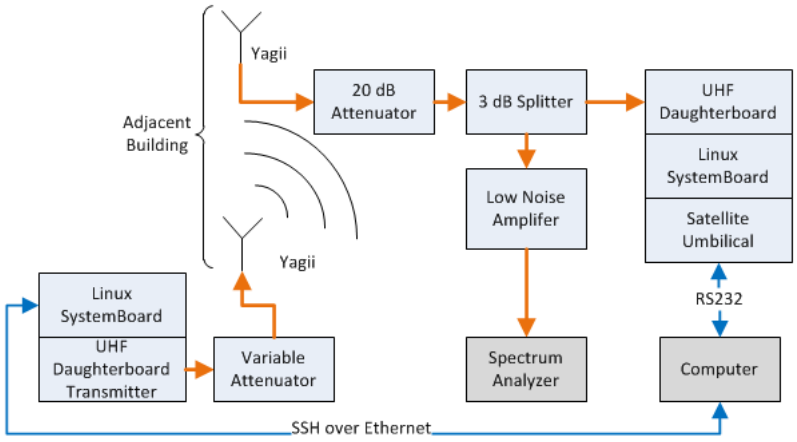

Figure 52: Indoor test setup with the variable attenuation moved to the TX side and 20 dB fixed attenuator on the RX side.

Table 20 shows a very strange result. Having an attenuator on the receive side appears to improve the receive sensitivity by around 10dB. Configuration E was done to show the Variable attenuator is not somehow defective, and that the same result is obtained with any attenuator on the front end. To gain some insight, the noise for the receiver is measured in various configurations. Figure 53 shows the noise floor in configuration A with the variable attenuator on the receive side set to the value that gives the sensitivity threshold. Figure 54 shows the noise floor in configuration C, where the variable attenuator is moved to the TX side. Figure 55 shows the noise floor in the configuration with a fixed attenuator on the RX side, and the variable attenuator on the TX side. Figure 56 is the noise floor show on the spectrum analyzer when the yagii antenna is attached directly to the LNA, and to the spectrum analyzer. This is essentially the noise in the room picked up through the antenna, which appears to be limiting the receive capability. Figure 57 is the noise floor for the UHF System in receive mode, with the coax from the UHF board going directly to the LNA, to the spectrum analyzer, This is the noise floor of the receive line from conductive noise sources internal to the board. Note for each case, the value shown in the graph is the amplified noise after the external LNA.

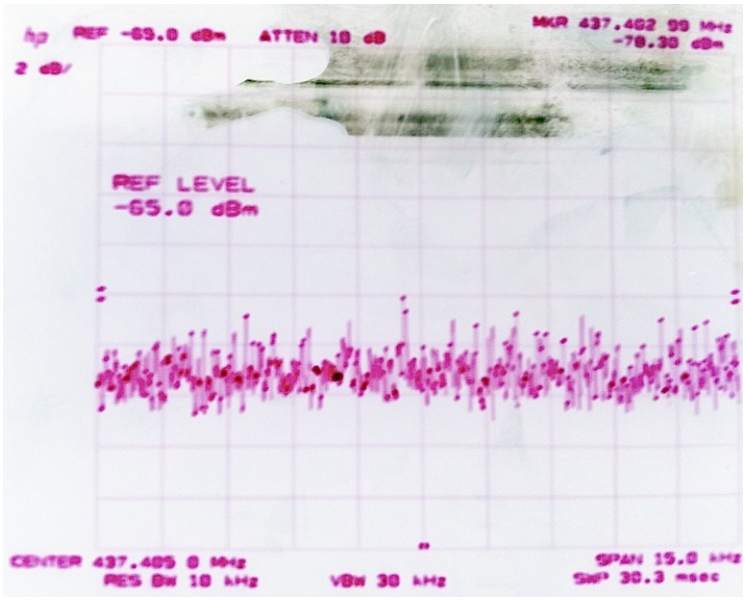

Figure 53: -120 dBm Noise Floor of Configuration A with Variable Attenuation at sensitivity threshold. 15kHz Span, 10kHz RBW, 2dB/Div.

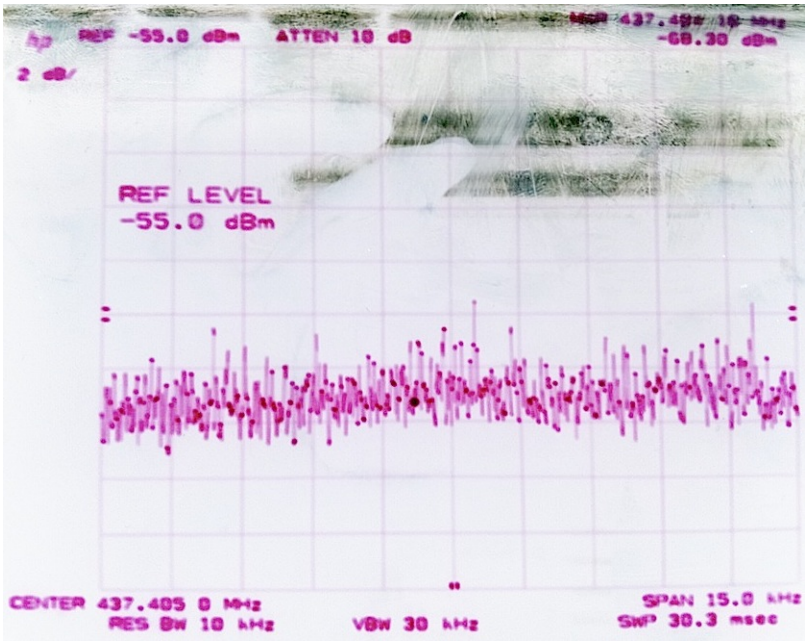

Figure 54: -110 dBm Noise Floor of Configuration C with Variable Attenuation at sensitivity threshold. 15kHz Span, 10kHz RBW, 2dB/Div.

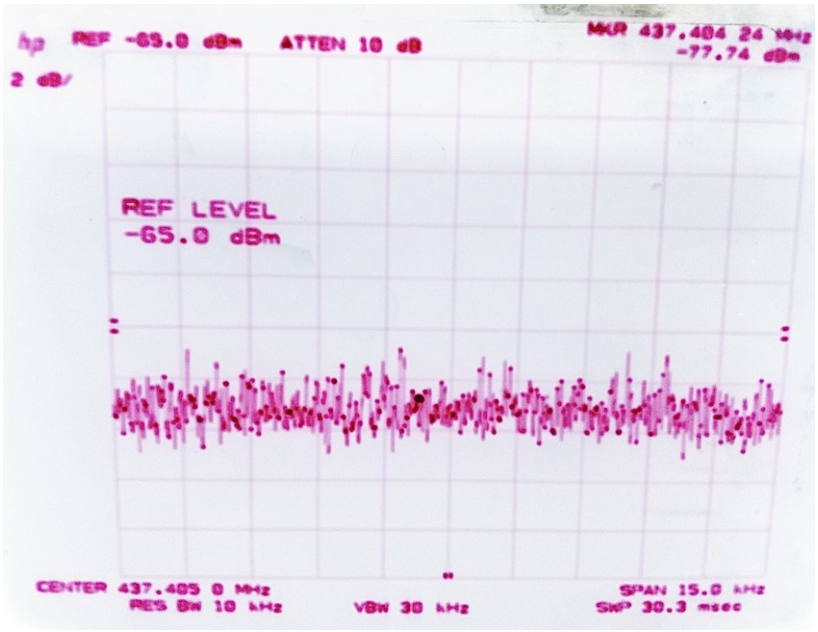

Figure 55: -120dBm Noise Floor of Configuration E with Variable Attenuation at sensitivity threshold. 15kHz Span, 10kHz RBW, 2dB/Div.

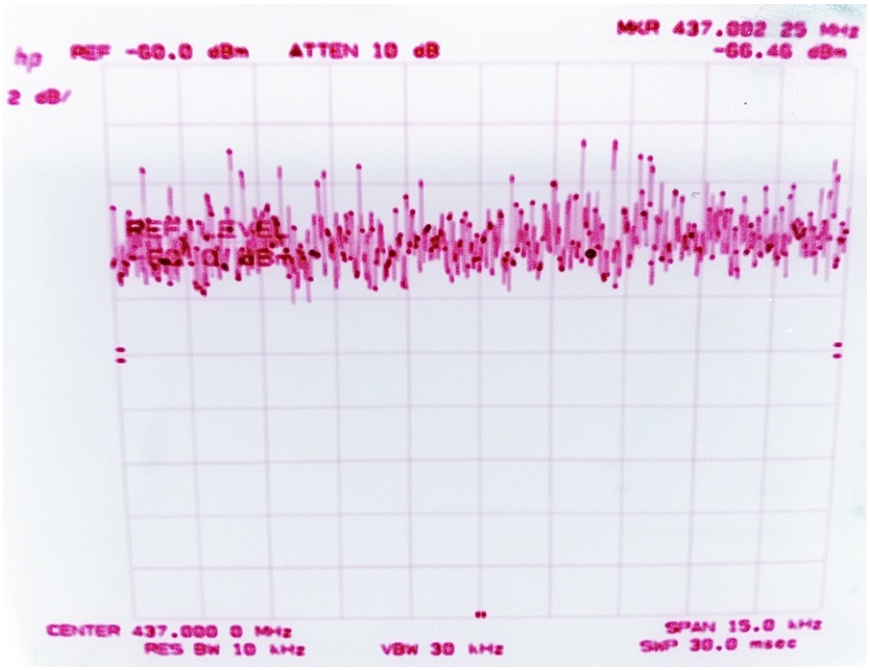

Figure 56: -108dBm Signal through Yagii Antenna with LNA. 15kHz Span, 10kHz RBW, 2dB/Div.

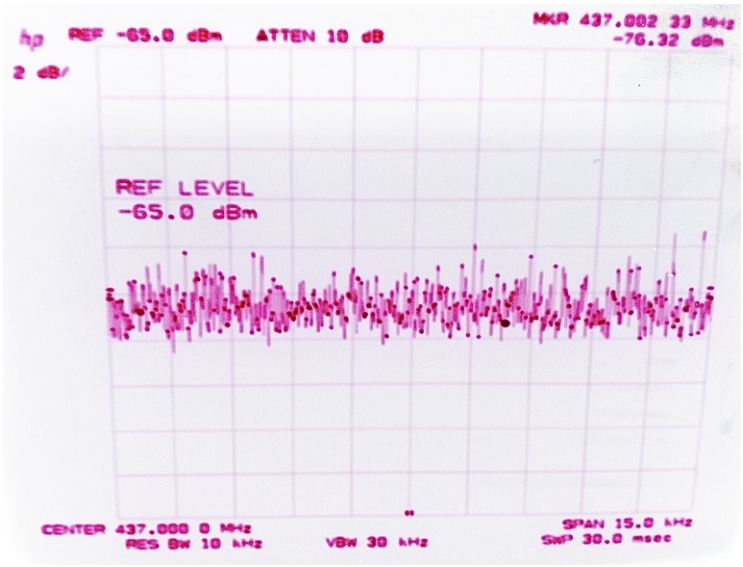

Figure 57: -118dBm Noise Floor of UHF Board in RX mode connected directly to LNA and Spectrum Analyzer. 15kHz Span, 10kHz RBW, 2dB/Div.

Table 20 summarizes the test results. There is a clear correlation between the noise floor level, and the measured receive sensitivity. It is reasonable to assume the 10dB drop in sensitivity is accounted for by a 10dB rise in the noise floor on the receive line. This phenomenon is both good and bad. It appears that the affective sensitivity of the system is dependent on and limited by the outside environment, as opposed to internal design issues. The drop in noise from from the Old Comm design [2], to the new UHF board is significant (I'm going to ignore the R5 Comm B Noise Floor Measurement since that must be a measurement error as it's below what the test setup can even measure). A comparison of those test cases show a 5 to 10 dB improvement in noise floor. All the setups in the table use a 10kHz RBW, allowing direct comparison. The noise temperature of the antenna is a critical determinant of the real world performance. As such, the scope of this thesis does not cover the antenna design, though the final system performance is heavily dependent on a properly implemented antenna, and any potential near field coupling with electronics.

8.7 Link Budgets for Various Data Rates

There are many different levels of link budgets, and simple ones are not always worse than very complicated ones provided they are based on empirical measurements. This section tried to generate a very simple link budget making conservative assumptions. After making the assumptions, two graphs are produced, one for uplink, and one for downlink. The key to making the simple budget accurate is it's based on real world performance numbers, with known signal strength thresholds for

Config	Description	NoiseFloor(dBm)
A	Attenuator on RX, from Figure 53	-120
C	Attenuator on TX, from Figure 54	-110
E	Fixed Attenuator on RX, Var Attenuator on TX, from Figure 55	-120
–	Noise Floor of signal through Yagii and LNA	-108
–	Noise Floor of UHF Board through LNA in RX Mode	-118
Old Comm	R4 Comm A Noise Floor	-108
Old Comm	R4 Comm B Noise Floor	-113
Old Comm	R5 Comm A Noise Floor	-113
Old Comm	R5 Comm B Noise Floor	-133
SpeccA	LNA to Spectrum Analyzer	-128

Table 20: Long Range Test 3: Noise floor measurement of the new UHF Comm in various configurations compared to the old design.

different data rates.

Parameter	Value	Unit	Notes
TX Power	30, 40, 46, 50	dBm	At output of RF Amp
G/S Antenna Pointing Loss	-0.6	dB	5 Degree Pointing Error
Line Losses	1	dB	Losses from U.FL to Antenna
TX Antenna Gain	19.4	dBi	Dual Phased Yagii's
Slant Range Path Loss	Variable	dB	20 Degree's above Horizon
S/C Antenna Pointing Loss	-7.6	dB	10 Degrees from Null
Antenna Polarization Loss	-3	dB	G/S Circularly Polarized
RX Antenna Gain	2.15	dBi	Monopole on S/C
Added Margin	3	dB	

Table 21: Simplified link budget for uplink using a Systemboard and UHF Daughterboard as the ground station interfaced to an external amplifier.

Table 21 shows the assumptions made for the uplink. Four different transmit powers were graphed together, with horizontal lines showing the signal strength threshold to properly decode, graphed against increasing altitudes of circular orbits. The Ground Station (G/S) Antenna Pointing Loss accounts for the inaccuracy of the stations tracking, whether it be mechanical, or poor orbital knowledge. A 5 Degree error is assumed, which is reasonable after several weeks in orbit after NORAD has provided solid Two Line Elements (TLE's) for accurate ground based orbit propagation. This error is likely larger immediately after launch. Line Losses account for any losses between where the Amplifier output power is measured, and the connection to the antenna. The 1dB is fairly arbitrary but reasonable. The Transmit (TX) antenna gain assumed the same Dual Phased Yagii's used on the current Cal Poly ground station, and have a 19.4 dBi gain. The Slant Range Path Loss is the X-Axis variable, and varies from 100km to 800km circular orbits. The actual slant range is calculated assuming the longest transmission distance attempted is 20 degrees above the horizon for each particular orbit altitude. The Spacecraft (S/C) Antenna Pointing Loss is based on the attitude

of the satellite relative to the ground-station. Assuming a simple monopole on the satellite, being 10 degrees from the Null gives a pointing loss of -7.6 dB for an ideal monopole, and acts as a worst case satellite attitude where the link can still be closed. Antenna Polarization Loss is -3dB since the G/S antenna is circularly polarized communicating to a linearly polarized antenna. In any attitude orientation, the Polarization Loss is -3dB. This is a worthwhile trade since two linear antenna communicating with each other are def if one is linearly polarized, while the other is horizontal, which is dependent on satellite attitude. The Receive Antenna Gain is assumed to be 2.15 dBi. In the literature, monopoles theoretically provide a gain of 5.15 dBi over an infinitely large ground plane, though this is an unreasonable assumption as our ground plane is electrical small. The size of the ground plane (CubeSat side panels and frame) will greatly affect the antenna impedance, and radiation pattern, as the peak gain will not be perpendicular to the antenna. The last item in the list is Margin, and is also arbitrarily set by the developer, and is currently shown as 3dB, since the other assumptions are believed to be conservative.

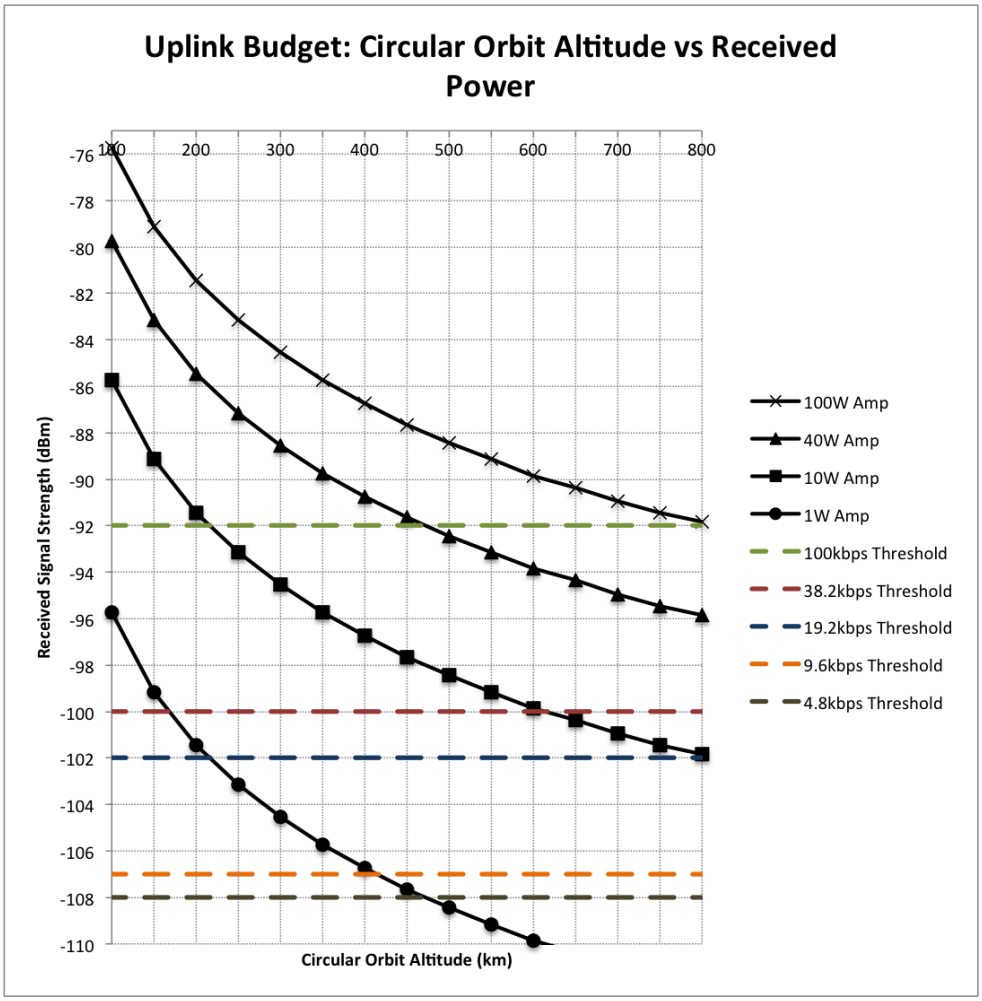

Figure 58: Conservative Uplink Budget graph showing four different transmit power levels, with signal strength thresholds for several data rates. Thresholds found inside a noisy Lab.

Figure 58 graphs the Uplink Budget results based on the assumptions in Table 21. The three critical parameters to pin down are the data rate, the transmit power, and the orbit altitude. The required signal strength for each data rate is shown to be directly dependent on the noise floor of the system, and in particular external noise. The thresholds shown in Figure 58 are considered to be worst case as these were measured in a lab, which is a very noisy environment. It's important to note that these thresholds may also depend on other components in a completely integrated system if they emit significant EMI that is coupled into the antenna. However, if the threshold can be measured on a complete system in a representative environment, this simple link budget would provide high confidence.

Table 22 show assumptions for the downlink, which are all the same as the Uplink, except the transmit powers are different, and the assumptions made for the threshold signal strengths shown in

Parameter	Value	Unit	Notes
TX Power	20, 24, 30, 33	dBm	At output of U.FL on Daughterboard
S/C Antenna Pointing Loss	-7.6	dB	10 Degrees from Null
Line Losses	1	dB	Losses from U.FL to Antenna
TX Antenna Gain	2.15	dBi	Monopole on S/C
Slant Range Path Loss	Variable	dB	20 Degree's above Horizon
G/S Antenna Pointing Loss	-0.6	dB	5 Degree Pointing Error
Antenna Polarization Loss	-3	dB	G/S Circularly Polarized
RX Antenna Gain	19.4	dBi	Dual Phased Yagii's
Added Margin	3	dB	

Table 22: Simplified link budget for downlink using a Systemboard and UHF Daughterboard as the ground station interfaced to an external LNA.

Figure 59. These thresholds assume the best case threshold of the hardware found using the faraday cage, largely because the ground antenna's are expected to have a very low noise temperature since they are high gain, high quality, and pointed directly at the sky. Additionally, an external, low noise pre-amplifier at the base of the antenna will improve the Noise Figure of the system significantly. The actual performance of the system will likely be better than the faraday cage test due to the Pre-Amp on the front end.

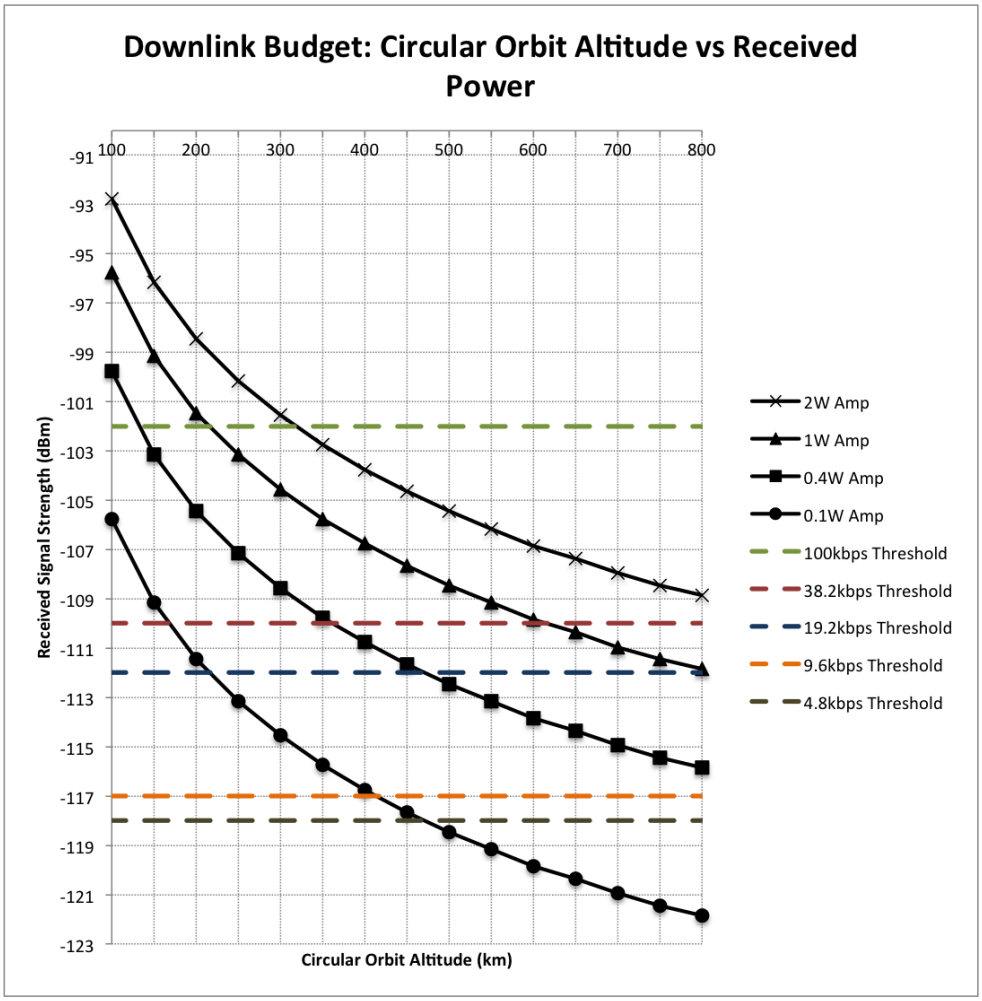

Figure 59: Conservative Downlink Budget graph showing four different transmit power levels, with signal strength thresholds for several data rates. Thresholds found inside lab using faraday cage. These thresholds are expected to be better than the spacecraft side due to the pre-amplifier, and lower noise level since the antenna's are pointed directly at the sky.

8.8 Flight Unit Qualification Test Setup

This section will describe a check-out setup PolySat can use on all its satellites to ensure the UHF System will work reliably on orbit, and determine early in development if there are any compatibility issues. A key to understanding the performance is to know the actual sensitivity of the system, which we've seen with the Systemboard and UHF Daughterboard combination is dependent on the external environment, and the final antenna configuration relative to the system itself. It's important to get sensitivity measurements with early revisions of hardware incase there are compatibility issues so future revisions can address them without affecting the satellite development schedule.

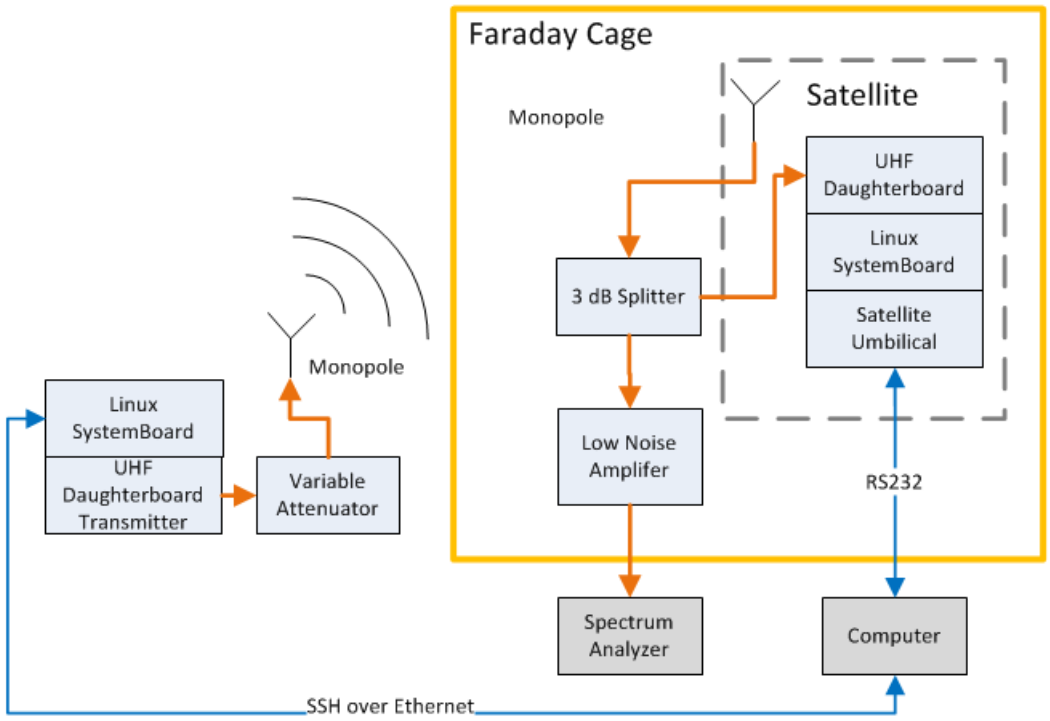

Figure 60: New Faraday Cage test setup. Transmits signal through the cage, and provides accurate sensitivity measurements in a more real world scenario. Useful for discovering any self jamming issues.

Figure 60 shows a diagram of a very useful test setup for understanding the performance of a complete system. The Faraday Cage is the same cage used in all previous test. The key difference is actually having the final antenna implementation on the receiving end, with the variable attenuation on the transmitting side. Doing so will give the actual performance of the system including any self jamming that may occur. The splitter will act as an attenuator, in the same way the variable attenuator improved the apparent sensitivity of the system by dropping the noise floor down to that seen on the board without an antenna, so this should be accounted for. The power actually received at the antenna will be highly variable with this test setup, so accurate measurements of each signal at the receiver using the spectrum analyzer are important. The same procedure used in Section 8.6 should be used to measure the received signal strength of every transmission until the threshold is found.

The best performance metric, however, would be accurate Receive Signal Strength Indicator (RSSI) readings from the transceiver chip, which we currently don't have working. Since a very clear correlation exists between the noise floor level on the receiver, and its ability to receive, using the RSSI to measure the noise floor will provide the most accurate performance characteristics since

the satellite is in a true flight configuration. It also has the added benefit of being very simple to test, since all that is required is placing the unit in a faraday cage, and turning it on to grab the reading in software. This makes it even easier to do throughout development while hardware is being developed and interfaced to the system.

9 Future Work

This section addresses future work to improve the design, or the lab's understanding if its performance characteristics. Improved performance knowledge goes a long way towards system optimization.

9.1 Switching Regulator

The current design uses only linear regulators on the RF daughterboard in an attempt to minimize noise in the power rail. It was unknown whether or not this would impact the sensitivity of the receiver, but was conservatively chosen as the power draw is relatively low for the transceiver. Now that the current design performance is well understood, a future revision could use a switching regulator if one is carefully selected and implemented in a way that doesn't not affect the performance, but provides power savings. The linear regulators are shown in Table 23. Only the devices that draw significant power are included, logic devices pull negligible current.

Regulator	**Devices**	**PowerDraw(mW)**	**Efficiency(%)**	**Total(mW)**
U10: LP3985-2.8	AX5042, TCXO,	70	65	108
U7: LP3985-3.0	RF2373	15	70	22

Table 23: Regulator power draws on the daughterboard when in receive mode.

There is an opportunity for power savings since these power draws are nearly 100% duty cycle while in orbit. There are a class of buck regulators designed to be very efficient at very low current levels. An example of one such device is the LTC3388. An efficiency of 90% is achievable at the current loads expected. The RF2373 is the low noise amplifier, and should probably be left with a linear regulator since its performance is critical, but the AX5042 would likely operate fine with a switching regulator.

Regulator	**Devices**	**PowerDraw(mW)**	**Efficiency(%)**	**Total(mW)**
U10:LTC3388	AX5042, TCXO,	70	90	78
U7: LP3985-3.0	RF2373	15	70	22

Table 24: Regulator power draws on the daughterboard when in receive mode using a switching regulator.

Table 24 shows the new power levels with the switching regulator in place. Going to the switching regulator saves 30mW of average power from the system. While this does not sound like much, if this type of power optimization is done throughout the satellite, significant savings begin to add up. It is important to test a variety of switching regulators, and verify they do not have a significant

impact on the receive sensitivity.

9.2 RSSI Functionality

The Receive Signal Strength Indicator is a common feature of most transceivers. The Axsem chip provides two RSSI readings of varying accuracy. The simplest reading requires no processing, while the other requires some C&DH processing, but is more accurate. The RSSI can measure the noise floor seen at the receiver. This data point is invaluable during satellite testing and integration to allow for debugging of any self EMC issues, which manifest themselves as a changing noise floor as a function of the satellite mode. The ability to take RSSI readings of the noise floor is currently functional, however, taking RSSI readings of the received signal has not yet been implemented. Sensing the received signal strength on orbit will provide a valuable data point to improve the accuracy of the link budget analysis.

9.3 Ground Station

PolySat has plans to utilize a Sytemboard and UHF Daughterboard combo to develop a new ground station. The Amateur Radio setup has worked well, but is limited in data rate. Additionally, some CubeSat missions should not be using the Amateur service, and instead will use the Experimental License through the FCC. Going Experimental will allow for higher data rates. Having the same hardware on the ground as on the satellite has the benefit of ensuring compatibility no matter what data rate or modulation scheme are chosen. The Systemboard will need to control the rotors for antenna pointing, and thus contain an orbit propagator base on TLE's obtained for NORAD. Various open-source orbit propagators have preliminarily been identified. In addition, an external power amplifier and Pre-Amplifier will be interfaced to improve the ground station performance. This will likely require modifications to some of the transmit and receive switch timing to optimize the link efficiency, and prevent any potential damage to the hardware itself. The performance is expected to be better than the Yaesu for the following reasons:

- The new UHF System has comparable performance at 9.6kbps as the Yaesu has at 1.2kbps in an ideal environment based on measurements from Ivan's thesis [2]. It's reasonable to assume the UHF System already outperforms the Yeasu in an ideal environment at 9.6kbps.
- The Yeasu requires manual control, and thus is housed inside the lab, which requires RF Cabling to be run to the roof. While high quality, the cable does exhibit losses. The new ground station is entirely housed inside a weather proof box on the roof at the base of the antenna,

dramatically shortening RF cable length. The interfaces are simply an ethernet cable and a wall plug for power.

- MixW decodes 9.6 kbps signals from amateur satellites using G3RUH FSK. This approach scrambles the data as a work-around for bandwidth limitations within 9600bps amateur radio transceivers. The downside, is this mode requires a Bit Energy to Noise Spectral Density (Eb/No) of 18dB, compared to 9.6dB for GMSK. Eliminating G3RUH FSK on the ground with something that can decode GMSK theoretically improves the link by 8.4 dB.

An improvement over the current downlink budget on the order of 10dB is not unreasonable by going to a new ground station.

9.4 Forward Error Correction

The AX5042 supports Forward Error Correction using a Convolution Code with parameters R=1/2 K=5. While this was briefly played with, a high packet drop rate was seen. FEC is a low priority at the moment, but eventually having this capability could be useful for applications where the link is very near the fringe of being operational, such as very high orbit missions, or allowing lower transmit powers on the spacecraft due to power budget issues.

9.5 Dynamic Data Rates

A nice feature of the software controlling the AX5042 is the ease with which RF parameters in the radio can be changed. The underlying infrastructure exists to allow dynamic programming of the Carrier Frequency, Modulation Scheme, and Data Rate. This holds great promise for link optimization during passes by starting with a lower data rate at the horizon, and increasing the data rate as the satellite passes overhead. Tuning the transmit power prior to launch based on the altitude and required data rate will also have a dramatic impact on the power budget, since the transmitter is generally among the highest power consumption device. The ability to get away with a 100mW transmitter vs a 1 or 2 Watt transmitter provides dramatically more payload power. The data rates shown are only those with measured sensitivities. It's pretty clear at lower altitudes, data rates above 100kbps appear feasible. Producing more sensitivity measurements in an operational environment will produce accurate link budget graphs with a higher fidelity of data rate changes for better link optimization. These graphs shown in Figures 61, 62, and 63 only account for altitude, and ignore RSSI measurements. The assumptions for these link budgets are shown in Table 25, and are the same as before. If RSSI readings of the signal strength coming in could be measured, that could

be fed into the control loop as well. Since rotation rates are generally slow for a tumbling cubesat, the RSSI would give an indication of sub-prime antenna point during communication, and the data rate could be lowered to accommodate the lower signal strength until the RSSI value improves. Depending on the accuracy of the RSSI, that could be relied on for data rate changes, and not worry about on-orbit propagators. In this case, the data rate would always start at 9.6kbps, and increase based on RSSI rather than altitude. The advantage of this method is it's orbit independent. However, measures for discarding incorrect RSSI readings need to be built in. If the UHF System were to get into any weird state, a variety of reset mechanisms are built in, and after a soft reset or power cycle, the satellite recovers in a known state with a "fail safe" mode.

Parameter	Value	Unit	Notes
TX Power	20, 24, 30, 33	dBm	At output of U.FL on Daughterboard
S/C Antenna Pointing Loss	-7.6	dB	10 Degrees from Null
Line Losses	1	dB	Losses from U.FL to Antenna
TX Antenna Gain	2.15	dBi	Monopole on S/C
Slant Range Path Loss	Variable	dB	From 20 to 160 degree elevations
G/S Antenna Pointing Loss	-0.6	dB	5 Degree Pointing Error
Antenna Polarization Loss	-3	dB	G/S Circularly Polarized
RX Antenna Gain	19.4	dBi	Dual Phased Yagii's
Added Margin	3	dB	

Table 25: Simplified link budget for downlink using a Systemboard and UHF Daughterboard as the ground station interfaced to an external LNA using a variable downlink method.

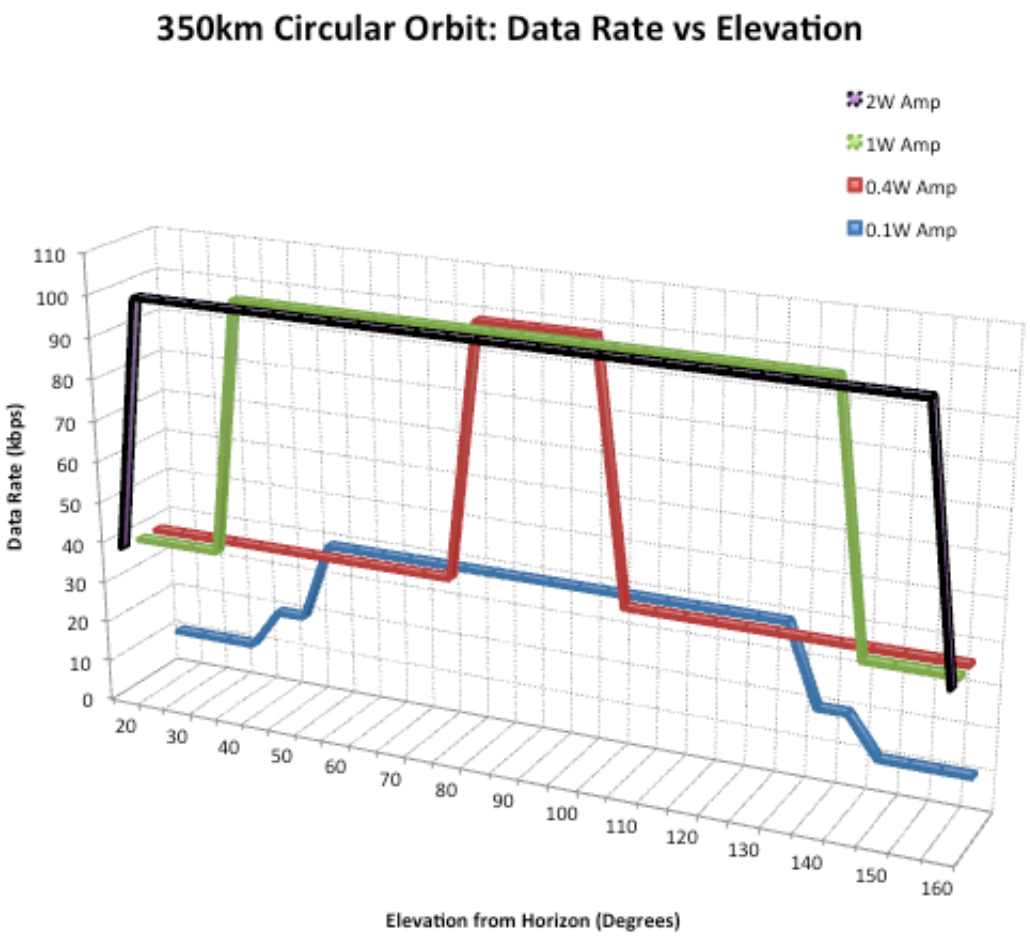

Figure 61: Graph of Data Rate versus Elevation for a 350km circular orbit for transmits powers of 0.1, 0.4, 1 and 2W

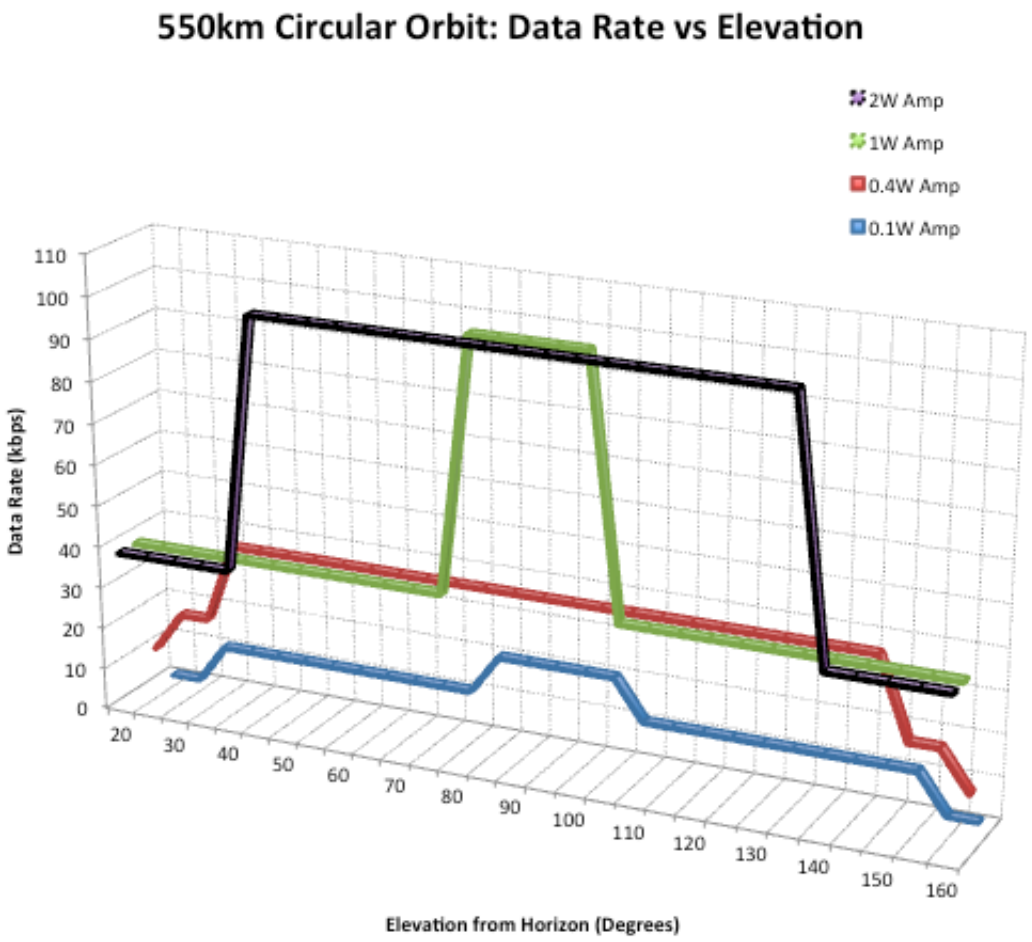

Figure 62: Graph of Data Rate versus Elevation for a 550km circular orbit for transmits powers of 0.1, 0.4, 1 and 2W

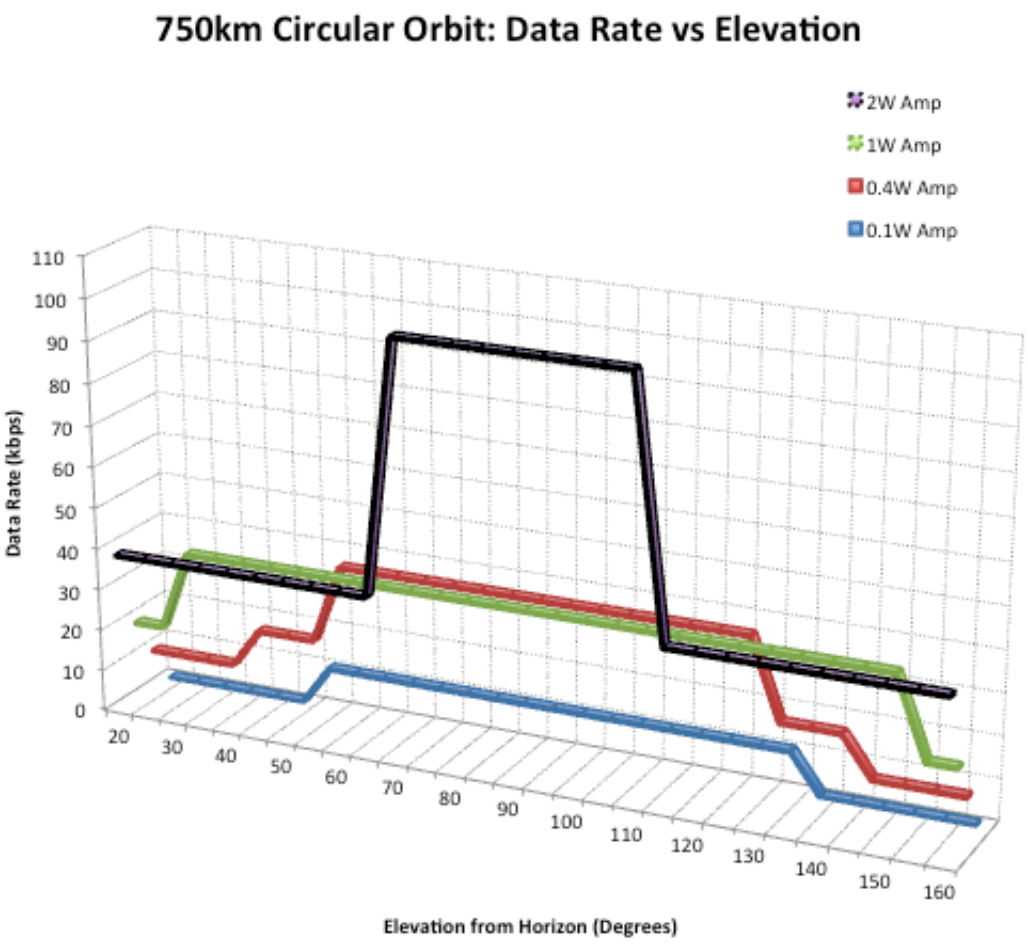

Figure 63: Graph of Data Rate versus Elevation for a 750km circular orbit for transmits powers of 0.1, 0.4, 1 and 2W

Bibliography

1 Klofas, Bryan. ”Improving Receive Sensitivity of the CPX Bus.” Cal Poly Senior Project. June 2008.

2 Bland, Ivan. ”Receive Sensitivity Characterization of the PolySat Satellite Communication System.” Cal Poly Masters Thesis. March 2010.

3 Huera, Derek. “Development of a Highly Integrated Communication System for use in Low Power Space Applications.” Cal Poly Masters Thesis. April 2006.

4 Noe, Chris. ”Design and Implementation of the Communications Subsystem for the Cal Poly CP2 Cubesat Poject.” Cal Poly Senior Project. June 2004.

5 Day, Chris. “The Design of an Efficient, Elegant, and Cubic Pico-Satellite Electronics System.” Cal Poly Masters Thesis. December 2004.

6 Maxim IC. “MAX2640/MAX2641 Datasheet.” April 2007. Availible online at http://datasheets.maxim-ic.com/en/ds/MAX2640-MAX2641.pdf. Accessed 26 Feb 2008.

7 Arakaki, Dean. “Experiment 4: Noise Figure and 1dB Compression Point of an Amplifier Using the Vector Network Analyzer.” EE480 Lab Manual. Cal Poly Electrical Engineering Department.

8 Anritsu Application Note. “Noise Figure: Scorpion Option 4.” April 2000.

9 CC1000 Data Sheet. Available at http://www.ti.com.

10 Yaesu FT-847 User Manual. Available at http://www.yaesu.com/.

11 K. Nakaya, K. Konoue, H. Sawada, K. Ui, H. Okada, N. Miyashita, M. Iai, and S. Matunga. ”Tokyo Tech CubeSat: CUTE-1 – Design and Development of Flight Model and Future Plan.” *Proceedings of the 21st AIAA International Communications Satellite Systems Conference, Yokohoma, Japan, 2003*.

12 FCC. Part 97 - Amateur Radio. Available at www.arrl.org/part97-amateur-radio.

13 iCom IC-910H Brochure. Available at www.icomamerica.com/an/amateur/.